JACS
JOURNAL OF THE AMERICAN CHEMICAL SOCIETY

Article

pubs.acs.org/JACS

Nucleation is Second Order: An Apparent Kinetically Effective Nucleus of Two for $Ir(0)_n$ Nanoparticle Formation from $[(1,5\text{-COD})Ir^{I}\cdot P_2W_{15}Nb_3O_{62}]^{8-}$ Plus Hydrogen

William W. Laxson and Richard G. Finke*

Department of Chemistry, Colorado State University, Fort Collins, Colorado 80523, United States

Supporting Information

ABSTRACT: Nucleation initiates phase changes across nature. A fundamentally important, presently unanswered question is if nucleation begins as classical nucleation theory (CNT) postulates, with n equivalents of monomer A forming a "critical nucleus", A_n, in a thermodynamic (equilibrium) process. Alternatively, is a smaller nucleus formed at a kinetically limited rate? Herein, nucleation kinetics are studied starting with the nanoparticle catalyst precursor, [A] = $[(Bu_4N)_5Na_3(1,5\text{-COD})Ir^{I}\cdot P_2W_{15}Nb_3O_{62}]$, forming soluble/dispersible, B = $Ir(0)_{\sim 300}$ nanoparticles stabilized by the $P_2W_{15}Nb_3O_{62}^{9-}$ polyoxoanion. The resulting sigmoidal kinetic curves are analyzed using the 1997 Finke–Watzky (hereafter FW) two-step mechanism of (i) slow continuous nucleation (A → B, rate constant k_{1obs}), then (ii) fast autocatalytic surface growth (A + B → 2B, rate constant k_{2obs}). Relatively precise homogeneous nucleation rate constants, k_{1obs}, examined as a function of the amount of precatalyst, A, reveal that k_{1obs} has an added dependence on the concentration of the precursor, $k_{1obs} = k_{1obs(bimolecular)}[A]$. This in turn implies that the nucleation step of the FW two-step mechanism actually consists of a second-order homogeneous nucleation step, A + A → 2B (rate constant, $k_{1obs(bimol)}$). The results are significant and of broad interest as an experimental disproof of the applicability of the "critical nucleus" of CNT to nanocluster formation systems such as the $Ir(0)_n$ one studied herein. The results suggest, instead, the experimentally-based concepts of (i) a kinetically effective nucleus and (ii) the concept of a first-observable cluster, that is, the first particle size detectable by whatever physical methods one is currently employing. The 17 most important findings, associated concepts, and conclusions from this work are provided as a summary.

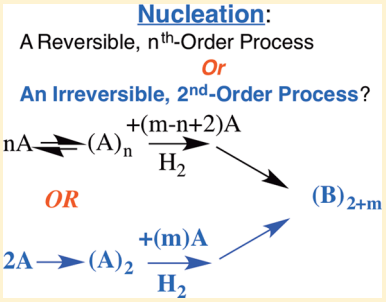

INTRODUCTION

The Generality and Hence Broad Importance of Nucleation and Growth Across Nature. Nucleation and growth phenomena are essential components of phase changes for many chemical and physical systems in areas as diverse as materials science, atmospheric and climate research,[1,2] degenerative neurological diseases,[3,4] and many other important systems throughout nature. It is, therefore, critical to have an accurate mechanistic model of nucleation—those crucial first events governing the formation of the new phase[5]—to be able to rationally design reproducible, size- and shape-specific syntheses of nanoparticulate and larger systems formed by nucleation and growth processes. Unfortunately, a consensus view of nucleation, and especially its mechanism, has not emerged. Indeed, Liu has commented that "Nucleation, in particular its mechanism, continues to be one of the most poorly understood and disputable phenomena in the past half century".[5] In nanoparticle chemistry in particular, the mechanism of nucleation has been a long sought goal,[6] given that nucleation greatly influences[5] the size, shape, and resultant electronic, optical, and catalytic properties[6,7] of the resultant new phase. A kinetic and mechanistic understanding of nucleation is, therefore, a critical gap in our fundamental understanding of phase changes throughout nature.

A Brief Review of Classical Nucleation Theory and Its "Critical Nucleus" Concept. Classical nucleation theory (CNT) is the first—and currently still the most popular—theoretical model for nucleation.[6] CNT is, inherently, a thermodynamic, equilibrium-based model in which n equivalents of monomer, A, are implied to be in associative equilibria up to a putative "critical nucleus", A_n, that is then postulated to be stable enough to grow rather than dissociate back to A. CNT postulates a balance of thermodynamic forces of favorable bonding or other associations between the precursor A vs the increasingly unfavorable interfacial surface energy associated with the creation of a new interface between the nucleus, A_n, and the solution. CNT has been widely used to try to explain nucleation[6] since its earliest formulation by Volmer[8,9] and Becker and Döring.[10] LaMer then adopted CNT as part of his widely cited, but still little supported, "burst nucleation and diffusion-controlled particle growth" mechanism dating back to the 1950s.[11] One fundamental problem with CNT from a kinetic perspective is the statistical improbability of a kinetically facile, higher-order, reversible $n > 3$ nucleus; true termolecular (concerted) reactions being rare and documented primarily only in gas-phase reactions.[12]

Received: October 8, 2014
Published: December 5, 2014

dx.doi.org/10.1021/ja510263s | J. Am. Chem. Soc. 2014, 136, 17601–17615

Despite its widespread and continued use, CNT has proven unable to match experimental measurements of nucleation rate constants,[13] often being off by even up to 10^{6-10} in its predicted rate constants.[14−16] CNT appears to be best suited for systems such as hydrocarbon associations in the gas phase,[13,17] at high temperatures,[6] or for latex particle associations[18,19] in solution—what we will designate herein as weakly bonded (i.e., weakly associating) systems. Even then, nucleation is one of the few fields where predictions accurate within $\pm 10^{1-2}$ are considered "a major success".[20]

Furthermore, the theoretical "critical nucleus" of CNT has arguably never been actually detected as one expects since it is by definition the least stable, highest energy species that, therefore, would be a fleeting transient between the starting material and the final, phase-changed product.[6] Indeed, in 2001 Gasser and co-workers[21] noted at the time that "No experiment has ever directly measured the size of the critical nucleus" prior to their confocal microscopy studies of the weakly associating poly-12-hydroxy-stearic acid-stabilized poly(methyl methacrylate) sphere aggregations; those larger, and preformed latex particles being used as a *model* of nucleation and growth, albeit one of preformed particles and not atomic or molecular precursors (and, therefore, really a study on the nucleation of *aggregation*). On reflection, it is remarkable that CNT continues to be so widely employed despite overwhelming, recurring, and repetitive evidence that CNT fails in especially more complex systems in nature.[13−16,22] This statement applies especially to strongly associated (bonded) systems that are often not of the simple $n\mathrm{A} \rightarrow \mathrm{A}_n$ type such as the Ir nanoparticle system herein with its relatively strong Ir−Ir and probably Ir−H−Ir bonds, *vide infra*. For such more complex systems there is no compelling evidence that CNT can predict, much less quantitatively account for even *ex post facto*, experimentally measured nucleation rate constants.

The Distinction Between Strongly vs Weakly Bonding Systems—Plus the New Concept of a Kinetically Effective Nucleus. The inability to have a reversibly associating, $n\mathrm{A} \rightarrow \mathrm{A}_n$ type system up to the putative critical nucleus of CNT is expected to be especially pronounced in what we designate herein as strongly bonded (alternatively "strongly associating") systems.[6] Transition-metal nanoparticles, for example, formed from M^0_n nuclei (or very plausibly M−H species, *vide infra*)[6] will generally have M−M (or M−H−M) bond energies of ≥25−30 kcal/mol[23] (to ≥55−75 for M−H)[24] and, therefore, are unlikely to exist as rapidly reversible systems associating up to the theoretical "critical nucleus" postulated by CNT. In the case of Ir, each Ir−Ir in a nucleus contributes a stabilizing enthalpy estimated to be at least ∼26 kcal/mol[25] and each Ir−H an estimated 75 kcal/mol.[24] Especially if Ir−H−Ir or Ir−$(\mathrm{H})_2$−Ir bonds form, then the resulting binuclear nucleus almost surely never reverses as CNT requires and assumes. The possible reversible formation of a less strong Ir−Ir is less clear, since Ir−Ir and Ir−L (and other M−M and M−L, M = transition metal) bonds are of roughly equal bond dissociation energies (BDEs).[23] This in turn means that the presence of high concentrations of relatively strong binding, BDE ≥ 26 kcal/mol ligands, L, could in principle lead to reversible formation of a Ir_n ($n \geq 2$) kinetic nucleus.[26,27] These considerations again lead logically to the suggestion of M−H−M bonds in the rate-determining step of nucleation. In short, the above thermochemical analysis further supports our hypothesis that M−H−M may well be more generally involved in transition-metal nanoparticle nucleation processes.[6,28] If so, then such $\mathrm{M}_x\mathrm{H}_y$ or other kinetic intermediates along the nucleation pathway would be profound in signaling that CNT does not apply and should not be used, as the system is not a $n\mathrm{A} \rightarrow \mathrm{A}_n$ type system, since A is highly soluble so that CNT and its notion of supersaturation in A are inapplicable.

Our second hypothesis for some time now has been that, in at least strongly bonding/strongly associating systems (and maybe many if not most others), nucleation will generally be under kinetic control and not the equilibrium control implied by CNT. As part of the present work we in turn define the more readily experimentally measurable kinetically effective nucleus (KEN) and distinguish it from the theoretical, experimentally nondetectable, and hence elusive "critical nucleus" of CNT. We define the KEN as the observed reaction order in a kinetically demonstrated nucleation step, specifically the reaction order, n, in the assembling monomeric precursor A, in a kinetically demonstrated nucleation step, $[\mathrm{A}]^n$.

Noteworthy here is that the small, KEN will generally be below the detection limit or time resolution of most analytical methods, that is, even the KEN will generally be missed by most analytical methods.[6] Those physical methods will, instead and in general, detect what we introduce and define herein as the first observable cluster (FOC), a concept we return to in the Results and Associated Discussion section. The KEN will, then, generally be detectable only by determining the kinetics of the phase change under study. These new concepts will tend to be especially applicable in systems that are *not* of the simpler $n\mathrm{A} \rightarrow \mathrm{A}_n$ type (e.g., not hydrocarbon droplet formation in the gas phase from low supersaturation conditions[17]), but rather where more complex chemistry is involved, such as the $2\mathrm{A} + \mathrm{H}_2 \rightarrow 2\mathrm{B}$ system herein (*vide infra*).

The 1997 Finke−Watzky Disproof Based Ockham's Razor Obeying/Minimalistic Two-Step Mechanism: Slow, Continuous Nucleation Followed By Autocatalytic Surface Growth. In 1997, the Finke−Watzky (hereafter FW) two-step mechanism[29,30] was the first to quantitatively fit sigmoidal nanoparticle formation data with a chemically precise mechanism and associated experimentally testable rate law. The FW two-step mechanism consists of two pseudo-elementary[31] steps[29] defined by their balanced reactions of: (i) slow, continuous nucleation, $\mathrm{A} \rightarrow \mathrm{B}$ (rate constant, $k_{1\mathrm{obs}}$) and (ii) autocatalytic surface growth, $\mathrm{A} + \mathrm{B} \rightarrow 2\mathrm{B}$ (rate constant $k_{2\mathrm{obs}}$), where A equals the nanoparticle precursor (in the present case the precatalyst $[\mathrm{A}] = [(\mathrm{Bu}_4\mathrm{N})_5\mathrm{Na}_3(1,5\text{-COD})\mathrm{Ir}^{\mathrm{I}}\cdot \mathrm{P}_2\mathrm{W}_{15}\mathrm{Nb}_3\mathrm{O}_{62}]$) and B is the growing nanoparticle, $\mathrm{Ir}(0)_n$. The disproof based, Ockham's razor obeying, deliberately minimalistic FW two-step mechanistic model is supported by more than 700 kinetic experiments[6] conducted mostly on the prototype transition-metal nanoparticle formation system in Scheme 1. As such, the $\mathrm{Ir}(0)_n$ nanoparticle formation system in Scheme 1 is one of the best studied nucleation and growth systems available across nature.[6,29] Those studies have yielded

Scheme 1. Formation of $\mathrm{Ir}(0)_{\sim 300}$ From the $[(1,5\text{-COD})\mathrm{Ir}\cdot \mathrm{P}_2\mathrm{W}_{15}\mathrm{Nb}_3\mathrm{O}_{62}]^{8-}$ Nanoparticle Precatalyst Under Hydrogen and in the Presence of 1 equiv of Proton Sponge to Scavenge the H^+ Formed

$$300\ [(1,5\text{-COD})\mathrm{Ir}\cdot \mathrm{P}_2\mathrm{W}_{15}\mathrm{Nb}_3\mathrm{O}_{62}]^{8-} + 750\ \mathrm{H}_2 \rightarrow 300\ \bigcirc + 1\ \mathrm{Ir}(0)_{\sim 300} + 300\ [\mathrm{P}_2\mathrm{W}_{15}\mathrm{Nb}_3\mathrm{O}_{62}]^{9-} + 150\ \mathrm{H}^+$$

dx.doi.org/10.1021/ja510263s | J. Am. Chem. Soc. 2014, 136, 17601−17615

nine valuable mechanistic and synthetic insights summarized in a footnote for the interested reader.[32]

The limitations of the FW two-step mechanism are also discussed elsewhere for the interested reader, limitations that derive, ultimately, from the minimalistic and thus too simple nature of the kinetic model and the average rate constants, average size, and other average nanoparticle properties that result from the deliberately minimalistic, Ockham's razor obeying, kinetic model.[33]

However, of considerable significance is that the two steps of the FW two-step model define and describe precisely and chemically the respective steps of the slow, continuous nucleation and autocatalytic growth, even if primarily phenomenologically and even if via composite, pseudo-elementary[31] steps that oversimplify the true, underlying, multistep nucleation and growth process. The significance of such balanced chemical equations, and thus mechanistically well-defined, precise kinetic and mechanistic descriptors for the overall phase change, is hard to overstate. In their absence, confusion and convolution of concepts and words result, for example, seen in purely physical chemical or engineering models, as documented and discussed elsewhere.[34,35] The implied corollary here is that, ultimately, model building of *dynamic* chemical systems in science proceeds rationally best from, and therefore needs to rest upon, a foundation of initially minimalistic, disproof-based, mechanistic models.

Emerging Evidence that Nucleation May Often Be Bimolecular or Possibly Termolecular in More Complex Systems and the Alternative Hypotheses of Tetra- or Higher-Molecularity Nucleation. The simplest, first hypotheses that could describe the KEN include: unimolecular, bimolecular, termolecular (i.e., trimolecular, $3A \rightarrow 3B$ $(= (B)_3)$) or conceivably tetra- $(4A \rightarrow 4B$ $(= (B)_4))$ or even higher-order formulations of the nucleation rate-determining step. Note here again that since true, concerted termolecular reactions are seen primarily for only gas-phase reactions;[12] hence what is meant by the above net stoichiometric equations is that reversible, prior associative equilibria would somehow be involved and lead to the net pseudo-elementary steps shown above with their implied, for example, net third or fourth orders in the primary reactant, A.

Within these possibilities and for the case of nucleation of $Ir(0)_n$ nanoparticles as studied herein, the greatest "energetic/physical discontinuity" would seem to occur when the first 2 A (i.e., herein the first two Ir) or perhaps the first three A form the first one or two A–A bonds (herein the first one or two Ir–H–Ir or Ir–Ir bonds). That is, rate-limiting bimolecular nucleation step, $A + A \rightarrow 2B$, to an implied KEN of 2, makes intuitive sense in the case of relatively strongly bonding A–A such as transition-metal nanoparticle formation (as opposed to relatively weak bonding of, say, nucleation of hydrocarbon aggregation in the gas phase and where improved CNT models can reproduce nucleation rate constants to within a $\sim 10^{1-2}$ error).[17]

Not unexpectedly, therefore, hints suggestive of bimolecular or possibly termolecular nucleation are beginning to appear in the literature of phase changes across nature. Four cases of note are kinetic evidence in 1989 for approximately bimolecular to termolecular $(n_{obsd} \sim 2.2)$ nucleation in Gelatin R1 renaturation,[36] the detection of Ag_2 in the formation of $Ag(0)_n$ nanoparticles,[37] a 2012 XAFS study of the formation of rhodium nanocubes suggesting $Rh_{\sim 2-3}$ species (*vide infra*),[38] protein aggregative nucleation and growth where a nucleus of 2 is used[39,40] as well as evidence for bimolecular nucleation in H_2SO_4 droplet formation relevant to atmospheric chemistry.[1,41,42] Looking a bit closer at the Rh nanocube formation study by XAFS, a discontinuous jump from zero to between one and two in the first-shell coordination of rhodium is observed during nucleation, implying Rh_2 or Rh_3 within experimental error.[38] These XAFS results provide suggestive evidence consistent with an XAFS-average KEN of Rh_{2-3} within experimental error, although the needed definitive kinetic data unequivocally demonstrating bi- vs ter-molecular nucleation and thus the origins of the observed Rh_{2-3} and attempting to disprove higher-molecular nucleation hypotheses are currently unavailable. Note also that the author's claim that "a Rh_4 cluster acts as the critical nucleus species for the formation of the nanocubes" is arguably better interpreted as what we define herein as the FOC (*vide infra*). There is also suggestive, albeit not definitive, evidence for second-order $[Pt]^2$ kinetics in $Pt^{II}Cl_4^{2-}$ reduction by H_2 to form $Pt(0)_n$ colloids in sodium citrate plus NaOH aqueous solutions.[43]

A side note of some interest here is that there is also increasing evidence for metastable M_4 species as detectable (e.g., Pt_4 by QXAFS),[44] or isolable (e.g., $Ir_4H_4(1,5\text{-COD})_4$),[45] or catalytically active (e.g., Rh_4) species.[46] The QXAFS direct observation of Pt_4 is especially relevant to the present contribution since the FW two-step mechanism was employed in that literature study and provided an excellent fit to the initial nucleation and growth kinetics of the poly(*N*-vinylpyrrolidone)-stabilized $Pt(0)_n$ nanoparticles (formed from H_2PtCl_6 in EtOH under benzophenone or benzoin-sensitized irradiation). Such Pt_4 and other M_4 species could of course be readily formed from simple dimerization of two M_2 kinetically effective nuclei to give M_4 as the FOCs or perhaps by single metal (M) addition to an M_3 KEN. Pt_4 was designated by those authors as the "nucleus" in their work,[44] but the published evidence[44] does not allow one to distinguish between the observed M_4 simply being the FOCs rather than the more fleeting KEN. Even more relevant to the present study is the rapid reaction of the isolated, crystallographically and XAFS characterized, coordinatively unsaturated subnanometer cluster[45] $Ir_4H_4(1,5\text{-COD})_4$ under H_2 to yield $Ir(0)_n$. Given that this system rapidly grows without an induction period to give a highly catalytically active system,[45] it provides strong evidence that the KEN is $n \leq 4$ in at least such Ir systems such as the one studied herein (*vide infra*).

Also exceedingly interesting and tantalizing is the observation of key T_d symmetry, M_4 building blocks in achieving dense packing in growing systems such as quasicrystals.[47,48] Any M_4 system can be formed at least formally by a dimerization of dimers, $(M_2)_2$, although it remains to be determined what the nucleation rate-determining step and the implied KEN are in these intriguing processes.

A bottom line, then, post-examining the extant nucleation and growth literature across nature is that definitive kinetic evidence for even the reaction order of the rate-determining step of nucleation is lacking. Further lacking is the mechanistic insight necessary to uncover the true molecularity of nucleation. This gap in our knowledge of nucleation across nature exists despite the anticipated much broader implications and fundamental importance of establishing the true KEN in at least a few prototype systems.

A crucial conceptual point to raise at this juncture is the important distinction between the more readily determined reaction order in a precursor or precatalyst A, $[A]^n$, vs the true

molecularity of the rate-determining step of the underlying, more intimate nucleation mechanism. These will generally be the same only in the case where A is the assembling monomer, $nA \rightarrow A_n$. In the present case, where A = the precatalyst $(Bu_4N)_5Na_3(1,5\text{-COD})Ir^{I}\cdot P_2W_{15}Nb_3O_{62}$, we can, for example, write more intimate mechanisms that will exhibit apparent nucleation kinetics second-order in A, $[A]^2$, but via mechanisms termolecular in Ir at the rate-determining step of nucleation; so that apparent second-order kinetics would actually correspond to a termolecular reaction in [Ir] and, therefore, a KEN of 3. Nevertheless, the first job at hand is to measure precise enough nucleation kinetics, a considerable challenge in its own right, to determine the net reaction order in the precatalyst A, in the present case, A = $(Bu_4N)_5Na_3(1,5\text{-COD})Ir^{I}\cdot P_2W_{15}Nb_3O_{62}$ for the prototype case of $Ir(0)_n$ nanoparticle formation. In a subsequent study in progress we will return to the even more challenging task of distinguishing unequivocally bi- from termolecular nucleation, that is, distinguishing a KEN of 2 vs a KEN of 3.

The Prototype $[(1,5\text{-COD})Ir\cdot P_2W_{15}Nb_3O_{62}]^{8-}$ Precatalyst and Resultant $Ir(0)_n$ Nanoparticle Formation Systems Plus the FW Two-Step Mechanism and Kinetics Exploited Herein. We employ herein our well-established $(Bu_4N)_5Na_3(1,5\text{-COD})Ir\cdot P_2W_{15}Nb_3O_{62}$ precursor and nanoparticle catalyst formation, the system where the FW two-step mechanism of slow continuous nucleation and autocatalytic surface growth was discovered and developed.[29] When placed in acetone or propylene carbonate under ~40 psig hydrogen, the polyoxometalate supported, $(1,5\text{-COD})Ir^{+}$ containing precatalyst $[(1,5\text{-COD})Ir\cdot P_2W_{15}Nb_3O_{62}]^{8-}$ is reduced to form near-monodisperse (i.e., by definition $\leq \pm$ 15% size distribution)[49] $Ir(0)_{\sim 300}$ nanoparticles stabilized by the $P_2W_{15}Nb_3O_{62}^{9-}$ polyoxometalate, Scheme 1.

The $Ir(0)_{\sim 300}$ nanoparticles form a very active cyclohexene hydrogenation catalyst which, in turn, serves as a well-developed reporter reaction[29] in which the slow steps of nucleation and growth can be followed and their signal amplified, by using cyclohexene:Ir ratios $\gg$1. The development of the $Ir(0)_n$ catalyst is, then, followed by the uptake of hydrogen involved in the net cyclohexene plus H_2 to cyclohexane, catalytic reporter reaction,[29] Scheme 2. Importantly, controls checking the reporter reaction have been performed many times by following the cyclooctane evolution (Scheme 1) directly by GLC and by verifying the zero-order dependence on the [cyclohexene] required to ensure that the reporter reaction is fast and not rate determining and, therefore, working properly[29] (Scheme 2, vide infra).

Scheme 2. FW Two-Step Mechanism and Its Coupling to the Cyclohexene Reporter Reaction

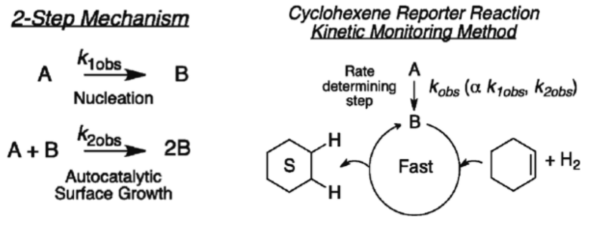

The H_2-loss kinetic data are then converted for convenience to their corresponding cyclohexene-loss curve, Figure 1, via the established 1:1 H_2 to cyclohexene stoichiometry.[29] The characteristic sigmoidal kinetic curve in Figure 1 is then fit to the integrated, analytic rate equation corresponding to the FW two-step mechanistic model, Scheme 2, using nonlinear-least-squares fitting, resulting in the desired nucleation rate constant k_{1obs} (as well as k_{2obs}) and associated fitting error estimates.

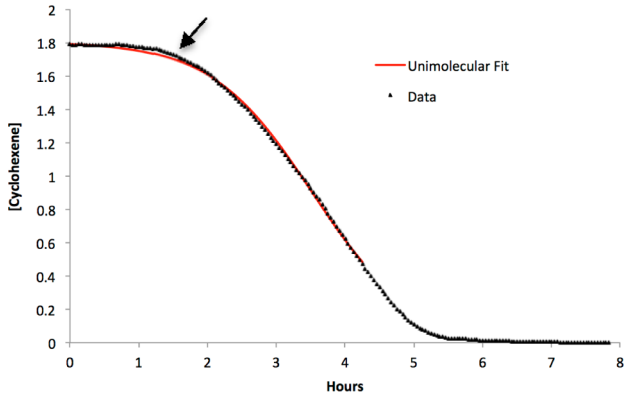

Figure 1. Representative sigmoidal kinetics for the $(Bu_4N)_5Na_3(1,5\text{-COD})Ir\cdot P_2W_{15}Nb_3O_{62}$ catalyst precursor in propylene carbonate under an initial 40 psig H_2 and coupled to the cyclohexene reporter reaction (Scheme 2). Also shown is the subsequent curve-fit to the FW two-step mechanism over the parts of the kinetic curve where the conditions necessary for the validity of the pseudo-elementary-step reporter reaction kinetic method are satisfied.[29] The arrow shows qualitatively where the first observable catalytically effective cluster, N*, can be detected.

Indicated qualitatively by the arrow shown in Figure 1, the end of the induction period is where hydrogenation catalysis is first detectable by our catalytic reporter reaction monitoring methodology.[29] That point designates the FOC by the catalytic reporter reaction monitoring method, what we previously called the catalytically effective cluster, N*.[50]

Addition of Bimolecular Nucleation to the FW Two-Step Mechanism: The Bimolecular-FW Two-Step Mechanism. In what follows, we formulate a bimolecular nucleation version of the FW two-step kinetic model. In doing so, we are treating the fundamental, conceptual simplest case where A is the assembling monomer and where bimolecular nucleation is an elementary step. Put another way, we will measure an *apparent* molecularity and *apparent* KEN size, *n*, as well as *apparent* bimolecular $k_{1obs(bimol)}$ rate constants in what follows, all under the assumption that A = $(Bu_4N)_5Na_3(1,5\text{-COD})Ir\cdot P_2W_{15}Nb_3O_{62}$ is the assembling monomer. Once we get to the experimental results, we will be careful to refer to what the experimental data actually provide, the observed reaction order in the precatalyst. Connecting that observed reaction order to the true molecularity of the nucleation step, and hence to the true size, *n*, of the KEN, can be done unequivocally only when the more complete, underlying mechanism is known with some certainty.

We have realized for some time now that true bi- or termolecular (or conceivably higher molecularity) nucleation could easily be kinetically hidden in the historical FW two-step kinetic model. This latter point follows since the concentration of the precursor, [A], is effectively constant to a precision of $\geq$99.95% (i.e., $[A]_t \cong [A]_0$) during the induction period and associated primary nucleation. Equation 1 shows the differential rate equation for the nucleation first step of the historical, unimolecular formulation for the FW two-step mechanism shown back in Scheme 2:

dx.doi.org/10.1021/ja510263s | J. Am. Chem. Soc. 2014, 136, 17601−17615

$$-\frac{d[A]}{dt} = k_{1obs}[A] \quad (1)$$

However, a higher reaction order, n, nucleation mechanism would have the kinetics shown in eq 2:

$$-\frac{d[A]}{dt} = nk_{1obs(n)}[A]^n \quad (2)$$

A bimolecular, $n = 2$, nucleation step with the rate constant $k_{1obs(bimol)}$, hereafter the bimolecular-FW two-step mechanism, is expected to show the kinetics given in eq 3, which includes the proper statistical factor of 2 that results from the 2A → 2B (= B_2) stoichiometry:

$$-\frac{d[A]}{dt} = 2k_{1obs(bimol)}[A]^2 \quad (3)$$

Combining eqs 1 and 3 yields eq 4, which provides the relationship between k_{1obs} and $k_{1obs(bimol)}$ for a $n = 2$ bimolecular nucleation mechanism:

$$\frac{k_{1obs}}{2[A]} = k_{1obs(bimol)} \quad (4)$$

In 2012 we provided initial kinetic evidence[51] suggesting that nucleation may be bimolecular or conceivably termolecular in a heterogeneous catalyst formation system in contact with solution starting with a different, but related, supported-organometallic heterogeneous precatalyst A = Ir(1,5-COD)Cl/γ-Al_2O_3. Under H_2 and in contact with acetone solution, this precatalyst forms the highly catalytically active, supported nanoparticle heterogeneous catalyst, B = $Ir(0)_{\sim 900}/\gamma$-Al_2O_3.[52] However, the nucleation data therein[52] are very noisy; nucleation rate constants generally being notoriously[53] hard to measure precisely as already noted. Nucleation mechanisms higher than bimolecular were briefly considered as part of that work but could not be definitively ruled out in that system. Hence, there remains a pressing need to establish the true nucleation reaction order and then the more intimate underlying mechanism and resultant implied molecularity and size of the KEN in a well-defined system.

Hence, herein we examine the nucleation rate constant, k_{1obs}, for the prototype[54] $(Bu_4N)_5Na_3(1,5\text{-COD})Ir{\cdot}P_2W_{15}Nb_3O_{62}$ precatalyst system forming $P_2W_{15}Nb_3O_{62}^{9-}$ polyoxometalate-stabilized $Ir(0)_{\sim 300}$ nanoparticles[55] over a 30-fold variation in concentration of the precatalyst. The observed data provide compelling evidence in support of second-order nucleation kinetics. The results are, therefore, of considerable interest and broader importance. They provide the currently best available disproof of the applicability of the CNT and its theoretical, equilibrium-based "critical nucleus" concept to at least the present $Ir(0)_n$ nanoparticle formation system. The results, in turn, lead logically to the experimentally-based kinetic concepts for nucleation provided herein of (i) the KEN and (ii) the FOC.

EXPERIMENTAL SECTION

The following ACS reagent grade compounds were obtained commercially and used as received: $NaBF_4$, $NaHSO_3$, $AgBF_4$, HCl (35%), H_3PO_4 (85%), Kryptofix [2.2.2.], $(Bu_4N)Br$, $Na_2WO_4{\cdot}2H_2O$, $NaClO_4$, KCl, Na_2CO_3, NaCl, $[(1,5\text{-COD})IrCl]_2$, $NbCl_5$, proton sponge, H_2O_2 (30%, <6 months old and stored at 5 °C), anhydrous Et_2O (HPLC grade, stored in a drybox), CH_3CN (HPLC grade, stored in a drybox over 3 Å molecular sieves), EtOAc (HPLC grade, stored in a drybox), propylene carbonate (99.9% Aldrich, stored in a drybox), CH_2Cl_2 (HPLC grade stored in a drybox), acetone (Burdick & Jackson <0.4% H_2O, stored in a drybox), cyclohexene (Aldrich, 99%) purified via a MicroSolv solvent purification system (Innovative Technology) using an activated γ-Al_2O_3 column under N_2 and stored in a drybox, NaOH, phenolphthalein (0.5 wt % in EtOH/H_2O), $(Bu_4N)OH$ solution (1.0 M in H_2O). Argon (99.998%) was used as received from Airgas, and high-purity H_2 (>99.5%) was passed through indicating moisture and O_2 scavenging traps (Trigon Technologies) before use in hydrogenations. Deuterated NMR solvents (CD_3CN, CD_3NO_2, and CD_2Cl_2) were obtained from Cambridge Isotope Laboratories in 1 g sealed glass ampules and were transferred into a drybox before use in NMR tubes sealed with rubber stoppers. D_2O was obtained from Sigma-Aldrich. All aqueous solutions were prepared using 18 MΩ deionized water from a nanopure filtration system.

INSTRUMENTATION

All pH measurements were made with a pH electrode standardized with two buffers (pH of 4.00, 7.00, or 10.01, bracketing the desired range). NMR spectra were obtained in 5.0 mm o.d. NMR tubes with the respective deuterated solvent prepared in a drybox and capped with rubber airtight stoppers. ^{31}P, ^{1}H, and ^{13}C NMR spectra were recorded on Varian Inova 300 or 400 MHz spectrometer at 21 °C. ^{31}P NMRs were externally referenced to 85% H_3PO_4. Air- and moisture-sensitive reactions were routinely preformed in a Vacuum Atmospheres drybox kept below 2 ppm of O_2 and constantly monitored by a Vacuum Atmospheres O_2 sensor, and air sensitive compounds were stored double bottled in the drybox.

(1,5-COD)Ir(CH_3CN)$_2BF_4$ Synthesis. This precursor was synthesized by the literature methods,[56] except BF_4^- was substituted for PF_6^- as described elsewhere.[57] The identity and purity of the product were established by ^{1}H NMR in CD_2Cl_2 and ^{13}C NMR in CD_3NO_2 in comparison to the published spectra.[56]

$K_6[\alpha$-$P_2W_{18}O_{62}]$ Synthesis. This parent Wells–Dawson polyoxometalate was synthesized by Nadjo's method,[58] but as detailed by Graham,[59] via that faster, higher yield, better atom economy and higher purity synthesis now available.[60] Purity of the product is 99.9% by ^{31}P NMR in D_2O in comparison to the published spectrum.[59]

$Na_{12}[\alpha$-$P_2W_{15}O_{56}]$ Synthesis. The synthesis of this lacunary polyoxometalate precursor was carried out by our new, improved methodology[61] for obtaining the highest known purity $Na_{12}[\alpha$-$P_2W_{15}O_{56}]$. A detailed procedure is provided therein,[61] one that must be followed to the letter to obtain the highest purity product. Briefly, a preparation by Droege et al.[62] was used except that the clay-like product was fully suspended during each of the five washing steps, including two added washes using deionized water that helped ensure all residual WO_4^{2-} is removed at a slight, <5% cost to the final yield. The observed purity of the $Na_{12}[\alpha$-$P_2W_{15}O_{56}]$ used in this work was ≥93–94% as determined by conversion to $(Bu_4N)_9P_2W_{15}Nb_3O_{62}$ and ^{31}P NMR of that product.[61]

$(Bu_4N)_9P_2W_{15}Nb_3O_{62}$ Synthesis. The $(Bu_4N)_9P_2W_{15}Nb_3O_{62}$ product was synthesized by our improved method[61] for preparing $(Bu_4N)_9P_2W_{15}Nb_3O_{62}$ (samples with 93–94% purity, by ^{31}P NMR in CD_3CN, were used in the experiments in the present work). Indeed, prior to the present nucleation kinetic studies several years of synthetic effort were expended improving the reliability and purity of this polyoxoanion precursor[61] with the goal of obtaining as precise and accurate nucleation rate constants, k_{1obs}, as possible. The main deviations from the prior Weiner[57] synthesis, as detailed elsewhere,[61] are (1) the use of 3.5 equiv of $NbCl_5$ in ∼5%

dx.doi.org/10.1021/ja510263s | J. Am. Chem. Soc. 2014, 136, 17601–17615

H_2O_2, (2) allowing the $Na_{12}[\alpha\text{-}P_2W_{15}O_{56}]$ added to that solution to stir for at least 1 h before continuing with the synthesis, (3) using extra $NaHSO_3$ (1.1 eq. vs H_2O_2) to destroy the additional H_2O_2, and (4) during titration of the $(Bu_4N)_5H_4P_2W_{15}Nb_3O_{62}$ intermediate with $(Bu_4N)OH$, the air free phenolphthalein end point was maintained for more than 6 h.

$(Bu_4N)_5Na_3(1,5\text{-COD})Ir\cdot P_2W_{15}Nb_3O_{62}$ Synthesis. The iridium catalyst precursor was synthesized by literature methods.[63] A drybox and other air-free methods were employed for this air-sensitive precatalyst.[63] The purity (~92%) and identity of the product were established by ^{31}P NMR in CD_3CN. Additionally, the quantitative 1:1 support of the $(1,5\text{-COD})Ir^+$ organometallic on the $P_2W_{15}Nb_3O_{62}^{9-}$ polyoxometalate was confirmed by a ^{31}P NMR monitored titration of $(1,5\text{-COD})Ir(CH_3CN)_2BF_4$ with $(Bu_4N)_9P_2W_{15}Nb_3O_{62}$ dissolved in CD_3CN, as recommended by Weiner[57] and as a check on the updated[61] $(Bu_4N)_9P_2W_{15}Nb_3O_{62}$ synthesis.

Preparation of Precatalyst Solutions. *Using Isolated $(Bu_4N)_5Na_3(1,5\text{-COD})Ir\cdot P_2W_{15}Nb_3O_{62}$ in the Main Studies.* In a ≤1 ppm of O_2, N_2-filled drybox, the $(Bu_4N)_5Na_3(1,5\text{-COD})Ir\cdot P_2W_{15}Nb_3O_{62}$ precatalyst along with 1 equiv of proton sponge was dissolved to final concentrations between 0.25 mM and 8.45 mM in a solution of 2.5 mL of propylene carbonate by agitating with a polypropylene pipet in 5 mL scintillation vial. After dissolution of the precatalyst, 0.5 mL cyclohexene was added and mixed for 30 s. Then, the solution was transferred to a new 22 × 175 mm disposable Pyrex culture tube containing a new 5/8 × 5/16 in. magnetic stir bar. The culture tube containing the precatalyst solution was then placed in a Fischer-Porter bottle modified with Swagelock TFE-sealed Quick-Connects, sealed, and transferred out of the drybox. That Fischer-Porter bottle was then used in an $Ir(0)_n$ nanoparticle formation kinetics experiment, *vide infra*, all according to our prior detailed descriptions.[29,30]

Using in Situ Generated $[(1,5\text{-COD})Ir\cdot P_2W_{15}Nb_3O_{62}]^{8-}$ in Control Experiments. For *in situ* generated $[(1,5\text{-COD})Ir\cdot P_2W_{15}Nb_3O_{62}]^{8-}$, in a ≤1 ppm of O_2, N_2-filled drybox equal molar amounts of $(1,5\text{-COD})Ir(CH_3CN)_2BF_4$ and $(Bu_4N)_9P_2W_{15}Nb_3O_{62}$ were added to separate 5 mL scintillation vials, and 1 equiv of proton sponge was added to the $(Bu_4N)_9P_2W_{15}Nb_3O_{62}$ sample. Next, 1 mL of propylene carbonate was added to each vial and the solutions were dissolved by agitating for 1−2 min with polypropylene pipettes which were then used to transfer each sample to a 22 × 175 mm disposable Pyrex culture tube containing a 5/8 × 5/16 in. magnetic stir bar. While stirring, the $(1,5\text{-COD})Ir(CH_3CN)_2BF_4$ solution was added dropwise by polypropylene pipette at a rate of ~1 drop every 2 seconds. A volume of 0.25 mL of propylene carbonate was used to rinse each scintillation vial, and the wash was added to the culture tube for a total of 2.5 mL propylene carbonate. Finally, 0.5 mL of cyclohexene was added to the culture tube and stirred for 30 seconds. The culture tube containing the precatalyst solution was then placed in a Fischer-Porter bottle modified with Swagelock TFE-sealed Quick-Connects, sealed, and transferred out of the drybox and used in an $Ir(0)_n$ nanoparticle formation kinetics experiment, *vide infra*, all according to our prior detailed descriptions.[29,30]

Monitoring the $Ir(0)_n$ Nanoparticle Formation Kinetics and Extraction of the k_{1obs} and k_{1obs}(bimol) Rate Constants. Nanoparticle formation reactions were monitored by the catalytic cyclohexene reporter reaction[29,30,52−54] shown back in Scheme 2. Specifically, the nanoparticle formation and concomitant cyclohexene hydrogenations were performed in a sealed Fischer-Porter bottle on a hydrogenation line described previously in detail elsewhere.[29] Precatalyst solutions prepared as described above were prepared in a drybox and then placed in a Fischer-Porter bottle modified with Swagelock TFE-sealed Quick-Connects, sealed, transferred out of the drybox, then attached via the Quick-Connects to the computer-monitored hydrogenation line. The $Ir(0)_n$ nanoparticle formation kinetics are followed by continuously monitoring the hydrogen pressure which is then converted to the solution cyclohexene concentration by the previously established 1:1 H_2/cyclohexene stoichiometry.[29]

Kinetic Data Analysis. The k_{1obs} and $k_{1obs(bimol)}$ rate constants were extracted from the sigmoidal cyclohexene concentration as previously described,[29] but without any vapor pressure correction during the crucial induction period since propylene carbonate has negligible vapor pressure at 22 °C (propylene carbonate being, therefore, deliberately chosen as the preferred solvent for these nucleation kinetic studies, one small but important key to the success of these studies). Origin 7 was used for nonlinear least-squares fitting of the cyclohexene data to the integrated rate equation for the unimolecular (eq 5)[29] or to the bimolecular (eq 6) formulations of the FW two-step mechanism (eq 6 is derived in the Supporting Information, as eq (S15) therein).

$$[\text{cyclohexene}]_t = \frac{\left(\frac{k_{1obs}}{k_{2obs(curvefit)}}\right) + [\text{cyclohexene}]_0}{1 + \left(\frac{k_{1obs}}{k_{2obs(curvefit)}[A]_0}\right) * e^{[k_{1obs} + k_{2obs(curvefit)} * [A]_0] * t}} \quad (5)$$

$$[\text{cyclohexene}]_t = \frac{k_{2obs(curvefit)}[\text{cyclohexene}]_0}{2k_{1obs(bimol,curvefit)}\{e^{(k_{2obs(curvefit)}[\text{cyclohexene}]_0 * t)} - 1\} + k_{2obs(curvefit)}} \quad (6)$$

In order to account for the stoichiometry of the reporter reaction, the appropriate mathematical derivations (eq (S15) of the Supporting Information) teach that the curvefit values for both $k_{2obs(curvefit)}$ and $k_{1obs(bimol,curvefit)}$ must be corrected by the [cyclohexene]/[Ir] ratio of ~1400 for solutions at 1.2 mM (see (S7−14) in the Supporting Information; see also a correction[64] involving a statistical factor of 2 in one equation derived as part of our previous work[51]).

Traditionally, fitting with the FW two-step mechanism has employed the cyclohexene-loss data only up through ca. half of the cyclohexene consumption in order to avoid the breakdown toward the end of the reaction on the assumption, required for the kinetic treatment[29] of $[A]_t \ll [\text{cyclohexene}]$.[30] However, at the higher concentrations of precatalyst, [A], necessary as part of this work, this practice under-fit the autocatalytic portion of the data (an example is available as Figure S1 in the Supporting Information). Hence, three-fourths of the cyclohexene data was used to fit all kinetic data, as shown for example in Figure 1.

RESULTS AND ASSOCIATED DISCUSSION

Kinetic Evidence Consistent with, and Supportive of, Second-Order Nucleation. A series of 18 $Ir(0)_n$ nanoparticle formation experiments were carried out in propylene carbonate using the isolated $(Bu_4N)_5Na_3(1,5\text{-COD})Ir\cdot P_2W_{15}Nb_3O_{62}$ catalyst precursor. These experiments spanned a ~30-fold concentration range of 0.25−8.45 mM. The kinetic curves

dx.doi.org/10.1021/ja510263s | J. Am. Chem. Soc. 2014, 136, 17601−17615

observed are all the expected sigmoidal nucleation and autocatalytic growth curves as seen in Figures 1 and 2.

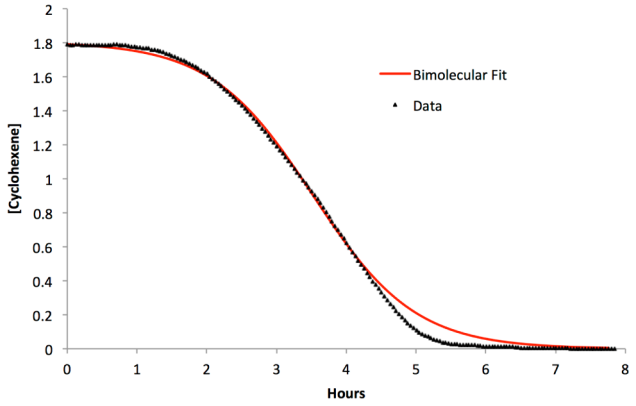

Figure 2. Cyclohexene (M) loss from the catalytic reporter reaction beginning with 1.5 mM $(Bu_4N)_5Na_3(1,5\text{-COD})Ir{\cdot}P_2W_{15}Nb_3O_{62}$ in propylene carbonate under an initial 40 psig H_2. Both the unimolecular FW and the bimolecular-FW kinetic models fit the data equally well and are statistically equivalent. Only the bimolecular fit is shown here because the fits using either eq 5 or 6 proved indistinguishable.

Fits of the kinetic data were obtained using both the unimolecular (eq 5) and bimolecular (eq 6) integrated rate equations. Those fits were indistinguishable both visually and statistically, producing the same coefficient of determination, R^2, and chi-squared per degree of freedom, Chi^2/DoF, statistical parameters. Therefore, just the bimolecular fit is shown in Figure 2. Furthermore, the k_{2obs} values calculated for both the unimolecular and bimolecular formulations are identical within experimental error.

The resultant k_{1obs} rate constants for the original unimolecular, formulation of the FW two-step mechanism are shown in Figure 3. The data demonstrate a linear dependence of the apparent rate constant k_{1obs} on the initial concentration

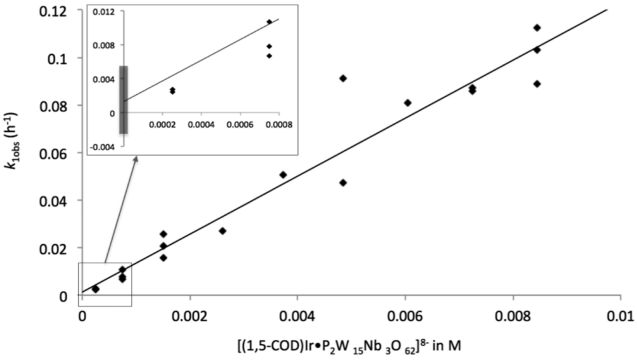

Figure 3. The k_{1obs} rate constant obtained by the traditional unimolecular A → B nucleation, two-step FW mechanism over a 30-fold variation in the concentrations of the initial complex, $(Bu_4N)_5Na_3(1,5\text{-COD})Ir{\cdot}P_2W_{15}Nb_3O_{62}$. The data show a clear linear trend with a linear least-squares regression line with a slope of $12.2(\pm0.8)\ h^{-1}\ M^{-1}$ (R^2 = 0.94; y-intercept = $1.3(\pm3.8) \times 10^{-3}\ h^{-1}$, from which $k_{1obs(bimol)} = 6.1(\pm0.4)\ h^{-1}\ M^{-1}$ can be readily calculated using the slope and eq 4. The inset shows a close up of the y-intercept, and the gray box indicates its uncertainty. Note that the y-intercept is $1.3(\pm3.8) \times 10^{-3}$, that is "0" within experimental error, arguing against any detectable heterogeneous or other parallel nucleation pathway within experimental error.

of the precatalyst, A = $(Bu_4N)_5Na_3(1,5\text{-COD})Ir{\cdot}P_2W_{15}Nb_3O_{62}$ catalyst precursor in propylene carbonate under an initial 40 psig H_2, implicating a second-order, or conceivably higher-order, *vide infra*, nucleation mechanism.

The apparent first-order rate constant, k_{1obs}, is related to $k_{1obs(bimol)}$ through the previous eq 4. A plot of $k_{1obs}/2*[A]$ vs the concentration of catalyst precursor yields $k_{1obs(bimol)} = 6.2(\pm1.3)\ h^{-1}\ M^{-1}$, and shows no discernible slope, Figure S2 of the Supporting Information, as expected if $k_{1obs(bimol)}$ is a true rate constant.

In addition, using the integrated rate equation for the bimolecular nucleation mechanism, eq 6 *vide supra*, we extracted the rate constant $k_{1obs(bimol)}$ this second way from the same series of experiments. A set of $k_{1obs(bimol)}$ rate constants result, Figure 4, which also show no further dependence on the initial concentration of the catalyst, precursor, again as expected if $k_{1obs(bimol)}$ is a true rate constant.

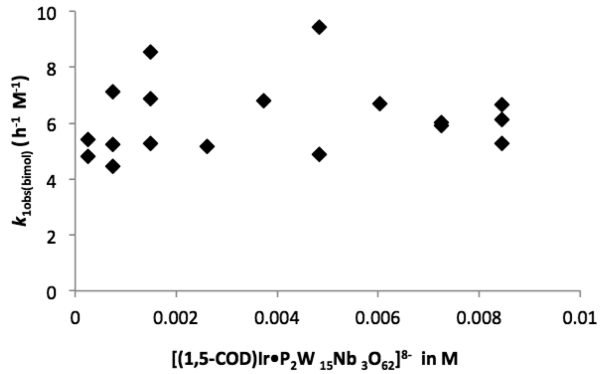

Figure 4. A plot of $k_{1obs(bimol)}$ vs the [A] = the initial $[(Bu_4N)_5Na_3(1,5\text{-COD})Ir{\cdot}P_2W_{15}Nb_3O_{62}]$ precatalyst concentration obtained by curve-fitting each kinetic run to the integrated rate equation for the bimolecular nucleation first step, A + A → 2B. The average value for the resultant rate constant obtained this way is $k_{1obs(bimol)} = 6.2(\pm1.3)\ h^{-1}\ M^{-1}$.

The derived rate constants from the unimolecular and bimolecular treatments are, as expected but still pleasingly, identical, including in their experimental error, $k_{1obs(bimol)} = 6.2(\pm1.3)\ h^{-1}\ M^{-1}$ for both. In addition, both treatments show no further concentration dependence of $k_{1obs(bimol)}$ within the stated fitting error of each treatment. The consistency of $k_{1obs(bimol)}$ validates the assumption of an effectively constant [A] during nucleation so that eq 1 holds, $d[A]/dt = k_{1obs}[A]$, even though eq 3, $d[A]/dt=2{\cdot}k_{1obs(bimol)}[A]^2$, describes more precisely the nucleation mechanism. Restated, the identity $k_{1obs}[A] = 2{\cdot}k_{1obs(bimol)}[A]^2$ is hereby established experimentally during the primary nucleation and induction periods where [A] is effectively constant.

The consistent $k_{1obs(bimol)}$ values, regardless of if they are obtained by eq 1 or 3, further act as an internal check that each equation has been properly implemented without mathematical or numerical errors, including application of the mathematically required correction of $k_{1obs(bimol,curvefit)}$ by the [cyclohexene]/Ir ratio as detailed in the Supporting Information. Overall, the results provide *prima facie* evidence that $k_{1obs(bimol)}$ is a rate constant, which in turn provides very strong evidence for rate-limiting, *second-order*, albeit not necessarily *bimolecular*, *vide infra*, nucleation in the prototype, polyoxoanion-stabilized $Ir(0)_n$ nanoparticle formation system.[29,54]

dx.doi.org/10.1021/ja510263s | J. Am. Chem. Soc. 2014, 136, 17601−17615

Control Kinetic Studies Using *in Situ* Generated [(1,5-COD)Ir·$P_2W_{15}Nb_3O_{62}$]$^{8-}$. Despite the quality and consistency of the above-obtained nucleation data, as a control and second check of the system and the kinetic data, additional kinetic studies were performed using [(1,5-COD)Ir·$P_2W_{15}Nb_3O_{62}$]$^{8-}$ generated *in situ* by adding the precursors (1,5-COD)Ir-$(CH_3CN)_2BF_4$ and $(Bu_4N)_9P_2W_{15}Nb_3O_{62}$. The kinetic results using the *in situ* formed precatalyst showed slightly more scatter but produced equivalent results within experimental error to those in Figure 3, $k_{1obs(bimol)} = 7.9(\pm 2.1)\ h^{-1}\ M^{-1}$ (as detailed in the Supporting Information, Figures S3−S4). A valuable feature of these controls is that they give us confirmation of second-order nucleation observations by two researchers, separated by ≥7 years, using two independent syntheses (isolated and *in situ* prepared) of the precatalyst material. Restated, the multiyear delaying in publishing this work that was required to obtain the improved reproducibility and purity[61] [(1,5-COD)Ir·$P_2W_{15}Nb_3O_{62}$]$^{8-}$ employed herein—with the goal of ensuring that we obtained the best precision nucleation rate constants possible—did not change the results within experimental error but did give rate constants ∼40% more precise. However, taking that extra time and care does give us high confidence in the resultant, second-order nucleation kinetics and resultant rate constants since these data proved reproducible by two separate researchers working completely independently as well as ∼7 years apart.

Even with the above-demonstrated consistency of the kinetic data over time and precatalyst samples, it is important to remember that $k_{1obs(bimol)}$ and all other rate constants herein must be viewed presently as apparent rate constants and the implied KEN of 2 as an apparent KEN. Restated, the more intimate mechanisms possible here remain to be tested and supported or ruled out, mechanisms more complex than the by design minimalistic, Ockham's razor obeying, now bimolecular FW two-step mechanism used to analyze the data. Only for a truly elementary step does it follow that second-order kinetics imply a molecularity of 2 (bimolecular) and, for the case of an elementary nucleation step, a KEN of 2.

However, and in short, the data in Figures 3, the accompanying Figure S2 of the Supporting Information, and Figure 4 do provide very strong evidence that nucleation is second order resulting in an apparent KEN of 2 in the classic, polyoxoanion-stabilized $Ir(0)_n$ nanoparticle formation system. If higher order nucleation can be ruled out next, then the evidence for at least second-order nucleation will be compelling, *vide infra*.

Explicit Testing and Disproof of the Alternative Hypotheses of Third-, Fourth-, and Higher-Order Nucleation. The evidence at this point is highly consistent with and supportive of second-order nucleation in the prototype system of the formation of $P_2W_{15}Nb_3O_{62}^{9-}$ stabilized $Ir(0)_n$ nanoparticles from [(1,5-COD)Ir·$P_2W_{15}Nb_3O_{62}$]$^{8-}$ under H_2 in propylene carbonate. However, disproof of all other reasonable alternative hypotheses[65] for the reaction order of nucleation is required to provide truly compelling evidence for or against second-order nucleation and to distinguish it from higher-order nucleation processes such as those implied by CNT. Noteworthy here is that experimental evidence testing and convincingly disproving all higher-order nucleation past second-order nucleation is nonexistent for nanoparticle catalysts save our own initial efforts[51] and rare if not unavailable for any other system in nature, depending on how one views the small number of literature reports that come the closest to accomplishing this important mechanistic task.[39−41,51] Third-, fourth-[6,46] and even higher net-order nucleation is certainly conceivable given the literature cited in the Introduction section. These important alternative mechanistic hypotheses are, therefore, addressed next.

As noted in the Introduction, net reaction third- and fourth-order nucleation would involve the stoichiometryies 3A → 3B and 4A → 4B, respectively. Note, again, that these would not be concerted processes; instead, these alternative hypotheses involve prior equilibria and a resultant rate law third or fourth (or conceivably higher, n^{th}) order in the concentration of A, $[A]^{\geq 3}$. The fact that $[A]_t \cong [A]_0$ during nucleation again allows us to use eq 2 to express the putative third- and fourth-order versions, namely eqs 7 and 8, respectively.

$$\frac{k_{1obs}}{3[A]^2} = k_{1obs(trimol)} \tag{7}$$

$$\frac{k_{1obs}}{4[A]^3} = k_{1obs(tetramol)} \tag{8}$$

We can, then and analogous to the first-order plot provided in Figure S2, Supporting Information, use eqs 7 and 8 for the third- and fourth-order nucleation hypotheses: does dividing the apparent rate constant k_{1obs} by $[A]^2$ (eq 7) or $[A]^3$ (eq 8) to yield $k_{1obs(trimol)}$ and $k_{1obs(tetramol)}$, respectively, followed by their plot vs the [A] = [$(Bu_4N)_5Na_3$(1,5-COD)Ir·$P_2W_{15}Nb_3O_{62}$], yield anything that could be construed as a flat line? Or, will such plots be clearly nonlinear beyond experimental error as one expects from the flat line in the second-order plots shown back in Figure 4?

Figure 5 shows the results for $k_{1obs(trimol)}$ obtained via eq 7 and this method. The strong, obvious curvature rather than a

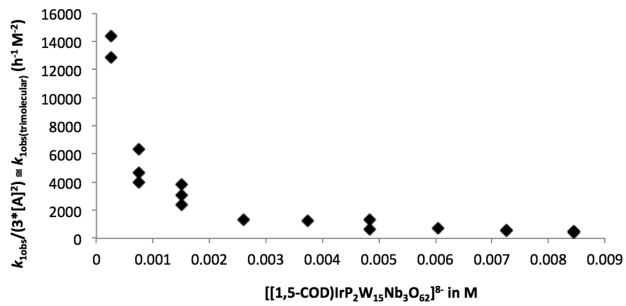

Figure 5. Third-order nucleation hypothesis plot according to eq 7 of $k_{1obs(trimol)} = k_{1obs}/(3[A]^2)$ vs [A] (=[(1,5-COD)Ir·$P_2W_{15}Nb_3O_{62}$]$^{8-}$). The curved, clearly nonflat plot and nonconstant $k_{1obs(trimol)}$ provides strong evidence against third order as well as higher order nucleation.

flat-line plot in Figure 5 is apparent. As such, Figure 5 (and even greater curvature using eq 8) provides strong evidence *against* nucleation processes with orders higher than 2.

The Absence of Detectable, Parallel-Path Heterogeneous Nucleation in the $(Bu_4N)_5Na_3$(1,5-COD)Ir·$P_2W_{15}Nb_3O_{62}$ System. The present studies make apparent that a special features of the present $(Bu_4N)_5Na_3$(1,5-COD)Ir·$P_2W_{15}Nb_3O_{62}$ system is that nucleation from this precatalyst is homogeneous within experimental error. Indeed, all the evidence to date,[29,66] including the relatively reproducible and acceptably precise $k_{1obs(bimol)}$ bimolecular nucleation rate constants obtained herein (that can still vary by a factor of 2 for a given run, however, see Figure 3), argue that nucleation is homogeneous (as opposed to the typically more facile

heterogeneous nucleation).[67] Already cited above was the intercept of the plot in Figure 3 which sets a upper limit to parallel, first-order heterogeneous nucleation (plus any other pseudo-first order nucleation) of $k_{1,hetero} \leq 0.001(\pm 0.004)\ h^{-1}$ under the reaction conditions.

In addition, in our 1994 studies we showed that increasing the glass surface area 2.5-fold by added glass beads—and the thereby deliberately uncontrolled addition of dust that those glass beads contain—has no detectable effect on the two-step k_{1obs} nucleation (or k_{2obs} autocatalytic growth) rate constants.[66] Those controls offer additional evidence that nucleation in the present $(Bu_4N)_5Na_3(1,5\text{-COD})Ir{\cdot}P_2W_{15}Nb_3O_{62}$ system is homogeneous without any kinetically detectable component of kinetically parallel, first-order heterogeneous or other net first-order nucleation pathways. Apparently, the relatively strong Ir−Ir (or Ir−H−Ir) bonding in the KEN is key, so that dust or other heterogeneous surfaces are not required to assemble the KEN.

Contrasting the desired homogeneous nucleation in the $(Bu_4N)_5Na_3(1,5\text{-COD})Ir{\cdot}P_2W_{15}Nb_3O_{62}$ system are the other, best literature studies to date of nucleation across nature, where dust and associated heterogeneous nucleation often dominate nucleation of (typically weakly bonded/associating) systems. A case in point is isonicotinamide organic crystal growth; there the authors find that dust particles—and resultant heterogeneous nucleation—dominates >2/3 of the otherwise impressive 144, repetitive crystallization trials.[68]

Additional Discussion and Implications of Second-Order Nucleation. *The Increased Separation of (Continuous) Nucleation and Autocatalytic Growth Provided by Second-Order Nucleation.* Figure 6 displays the idealized

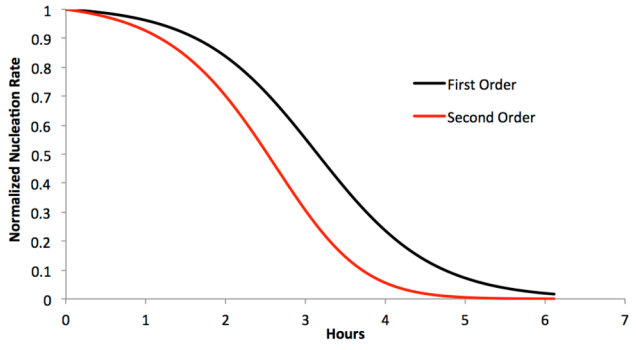

Figure 6. A comparison of the relative nucleation rates, $d[A]_n/dt$, for second-order $(-d[A]_n/dt = k_{1obs(bimol)}[A]_t^2)$ vs first-order $(-d[A]_n/dt = k_{1obs}[A]_t)$ nucleation of the otherwise identical reactions. Each set of rates is normalized to 1 in order to compare the subsequent time-course of the reaction post their maximum, initial nucleation rates. As expected, the rate of second-order nucleation decreases more quickly due to its squared precursor concentration dependence, $[A]_t^2$. Note, however, that nucleation is continuous until the precursor $[A]_t = 0$ at the end of the reaction, as was a main finding emphasized in even the title of our 1997 paper.[29]

nucleation rate as a function of time for the first- and second-order nucleation mechanism in a representative standard conditions $Ir(0)_{\sim 300}$ nanoparticle formation reaction with a concentration of 1.2 mM precatalyst. Figure 7 shows the resulting ratio of growth rate/nucleation rate over time for each case. To construct Figures 6 and 7, the rate constants from the representative kinetic run were extracted and paired with the implied $[A]_t$ based on those rate constants, $k_{1obs} = 0.018\ h^{-1}$,

Figure 7. Comparative plots of the ratio of the growth $(-d[A]_g/dt = k_{2obs(bimol)}[A]_t[B]_t)$ to nucleation rates for second-order $(-d[A]_n/dt = k_{1obs(bimol)}[A]_t^2)$ vs first-order $(-d[A]_n/dt = k_{1obs}[A]_t)$ nucleation. As expected but heretofore undocumented, second-order nucleation results in a greater separation of still continuous[29] nucleation from growth as a function of time. By the end of the ∼1 h induction period (e.g., as shown back in Figure 3), the ratio of the rates of growth to nucleation is already 270% larger in comparison to the same ratio for first-order nucleation.

$k_{2obs} = 904\ h^{-1}\ M^{-1}$, and for second-order nucleation, $k_{1obs(bimol)} = 6.1\ h^{-1}\ M^{-1}$, $k_{2obs} = 917\ h^{-1}\ M^{-1}$.

Figure 6 demonstrates an important feature of second-order nucleation: a greater separation of still slow, still continuous,[29] but now second-order nucleation, A + A → 2B, results in a more dramatic reduction in the nucleation rate as a function of time, $d[A]_n/dt$, defined by $k_{1obs(bimol)}*[A]_t^2$ (i.e., and in comparison to the first-order nucleation rate = $k_{1obs}[A]_t^1$). Figure 7 shows the resulting increased separation of nucleation and growth for second-order nucleation by plotting and comparing the ratio of the growth rate/nucleation rate for the second- vs the first-order nucleation mechanisms (i.e., and for the otherwise identical, net $Ir(0)_n$ formation reaction).

As Figures 6 and 7 detail, the increased separation of nucleation and growth in time is significant due to second-order nucleation. Specifically, ∼12 min into the reaction, which has an induction period of ∼60 min, the ratio of growth/nucleation is already 2.5 times larger compared to first-order nucleation. By 168 min, this ratio is 4 times as large, even though the reaction has only consumed ∼40% of the precursor, A. This rapid switch from appreciable rates of nucleation to primarily growth due to second-order nucleation is important in helping achieve the relatively small/narrow, ± 15% size dispersion[29] seen in the resultant nanoparticles (i.e., and when the FW two-step mechanism fits the kinetic data). In short, the second-order nucleation mechanism uncovered herein provides additional insight into why the resultant size distributions are relatively narrow; second-order nucleation provides a greater separation in time of the rates of (still continuous) nucleation vs autocatalyic growth.

Additional Discusion of the Needed Additional Concept of the First-Observable Cluster. Although there are many claims in the literature of observing and measuring the "critical nucleus", more generally what is probably actually measured is what we define herein as the FOC(s), that is, the first particle observable by whatever physical method one is using (i.e., and given its inherent sensitivity limits). This is distinct from KEN, which, being transient, requires nucleation kinetic studies in order to obtain evidence for the size (nuclearity) of that KEN.

A subcategory of such first-observable nuclei relevant to the present study is what we previously termed the "catalytically

effective nucleus",[50] N*. Based on the present work, a better name for N* is probably the "first observable catalytically effective cluster". The species N* is by definition the first catalytically competent cluster in transition nanoparticle autocatalytic growth and catalysis reaction observable by a detectable rate of catalysis such as a measurable drop in the H_2 pressure in Figure 3, *vide supra*.

Note here that, as the name "FOC" indicates, the physical method chosen (e.g., TEM, light scattering, XAFS, SAXS, etc.) and its detection limit are intimately tied to the (therefore somewhat variable) minimum-detectable size FOC. The more important point here, however, is that it is not the putative "critical nucleus" of nucleation theory that one is generally detecting by whatever physical method is being employed. Instead, it is the FOC.

In the case of the first observable catalytically effective cluster, N*, and for the $Ir(0)_n$ nanoparticle system employed herein, clusters in the range of 11−83 atoms, have been detected by both TEM and initial reaction product stoichiometry studies by GLC.[50] Noteworthy here is the conceptual confusion that would result if one (incorrectly) assumed these $Ir(0)_{\geq 18}$ were the "critical nucleus" of CNT, which in turn would then appear to demand a (thermochemically nonrealistic) reversible Ir(0) monomer addition/elimination up to that putative $Ir(0)_{\geq 18}$ "nucleus".

Mechanism-Based Equations for N and for the Final, Average Nanoparticle Size, D_f, Based on the Bimolecular-FW Two-Step Mechanism.* In 2008 we published the first, and to our knowledge still the only, mechanism-based equation for determining N* from the final average nanoparticle size, D_f, the initial concentration of precatalyst, $[A]_0$, the induction time, t_{ind}, and the rate constants for (at the time) unimolecular nucleation and autocatalytic growth, k_{1obs} and k_{2obs} herein, Scheme 2, *vide infra* (rate constants listed as just k_1 and k_2 in our 2008 publication).[50] That equation (no. 20 in our 2008 publication)[50] applies when the kinetic data for the system in question is well-fit by the historical FW two-step mechanism with its unimolecular nucleation step. Alternatively, if N* is known, the equation can be readily rearranged to give D_f in terms of N*, and the measurables $[A]_0$, t_{ind}, k_{1obs} and k_{2obs}.[50]

Now that we know that nucleation is empirically a second-order process well-fit by the bimolecular FW two-step mechanism, a rederivation of the equation for N* (and its rearrangement to an equation for D_f) is in order.

Those derivations, while straightforward, are provided in the Supporting Information for the interested reader. The only, but key, needed substitution vs the prior derivation[50] is in the equation for $[A]_t$ for the, now, bimolecular FW two-step mechanism, eq 9.

$$[A]_t = [A]_0 * \left[\frac{k_{2obs}}{2*k_{1obs(bimol)}(e^{(k_{2obs}*[A]_0*t)} - 1) + k_{2obs}} \right] \quad (9)$$

The use of eq 9 yields the desired eq 10 for N*, and if simply rearranged as before,[50] D_f, eq 11.

$$N^* = \frac{D_f^3 \pi \rho N_A}{6MW} * \left(1 - \frac{k_{2obs}}{2*k_{1obs(bimol)}(e^{(k_{2obs}*[A]_0*t)} - 1) + k_{2obs}} \right) \quad (10)$$

$$D_f = \frac{N^*6MW}{\pi \rho N_A \left(1 - \frac{k_{2obs}}{2k_{1obs(bimol)}(e^{(k_{2obs}*[A]_0*t)} - 1) + k_{2obs}} \right)}^{1/3} \quad (11)$$

It should be noted that the underlying derivation of these equations necessarily assumes the complete separation of nucleation and growth in time;[50] rigorously this would mean that no additional nucleation would occur past the induction period that determines N*. This assumption is never 100% true, as nucleation is continuous as we first experimentally determined in 1997[50] and as is obvious from the rate law for nucleation uncovered herein, $-d[A]/dt = k_{1obs(bimol)}[A]_t^2$), which teaches that nucleation slows but never stops and therefore is continuous until [A] = 0, at which time the nanoparticle reaction is over. But, a sizable separation of nucleation and autocatalytic growth is a pretty good approximation in the case of second-order nucleation, as the previous Figures 6 and 7 demonstrate.

In short, a high degree of separation of nucleation and growth in time should be apparent before employing eqs 10 and 11. However, and in that case, the fundamental value of the above mechanism-based equations is that they permit computation of the first observable catalytically effective cluster, N* or, alternatively, allow one to calculate the average final nanoparticle size, D_f, if a transferrable N* is known and the measurables $[A]_0$, t_{ind}, $k_{1obs(bimol)}$ and $k_{2obs(bimol)}$ are known.

A Rational, Mechanism-Based Treatment of Size Distributions vs Time Is Now Possible. Significantly, now that the second-order nucleation FW two-step mechanism is in hand, it is finally possible to undertake the additional, badly needed experimental studies and modeling simulations required for a rational, mechanism-underpinned analysis of nanoparticle size distributions vs time. That needed work is in progress and will be reported in due course.

CONCLUSIONS

The most important findings from this study, plus the new associated concepts, are summarized below as a bulleted list:

- Experimentally, nucleation is second order in at least the relatively strongly bonding, prototype nanocluster formation system of $Ir(0)_n$ nanoparticles studied herein with its strong, ca. 26 kcal/mol Ir(0)−Ir(0) bonds to ca. 75 kcal/mol Ir−H−Ir bonds.[25]
- The present work is, therefore, an important experimental demonstration that nucleation is under kinetic, not thermodynamic, control in at least the relatively strongly bonded $Ir(0)_n$ nanoparticle formation system studied herein.
- The demonstration in 1997 that nucleation is slow and continuous,[29] and not a "burst" phenomenon as the 1950s LaMer mechanism postulated,[11] is upheld by the present studies and is, in hindsight, a seminal finding in nucleation and growth studies across nature.
- CNT along with its equilibrium-based, theoretical concept of a "critical nucleus", A_n, formed from the reversible association of n momoners of A, is therefore disproven for the present $Ir(0)_n$ nanoparticle formation system. Restated, CNT is simply not applicable to the present nanocluster formation system until and unless such time as CNT is able to predict an Ir_{2-3} "critical nucleus" for this system (which, in CNT language, corresponds oddly to a critical nucleus of 1−2, not 2−3).

dx.doi.org/10.1021/ja510263s | J. Am. Chem. Soc. 2014, 136, 17601−17615

The failings of CNT are extensive, well-documented,[13−16,20,29] and therefore merit careful consideration by anyone claiming—incorrectly!—that CNT can be used for at least transition-metal and other complex nanoparticle nucleation systems and associated calculations or simulations.

- A new concept of the KEN is needed and therefore postulated as part of the present work. The apparent KEN for $Ir(0)_n$ nanoparticle formation, under the conditions of the present studies and based on the demonstration of second-order nucleation kinetics, is an apparent KEN of 2. The caveat here is that only when the underlying more intimate mechanism of nucleation when beginning with $(Bu_4N)_5Na_3(1,5\text{-COD})Ir\cdot P_2W_{15}Nb_3O_{62}$ is known, will the true molecularity of nucleation—and thus the true vs the apparent KEN—be known. However, from all the more intimate kinetic schemes for nucleation that we have been able to write at least to date, a KEN of between 2 and 3 (i.e., ≤ 3) is indicated.
- The evidence from the literature cited in the introduction pointing toward a KEN of 2−3 argues strongly for the potentially much broader applicability of the present results to nucleation and growth phenomenon across nature. The known systems at present where a KEN = 2−3 now include the present system, heterogeneous supported nanoparticle catalyst formation,[51] $Rh(0)_n$ nanoparticle formation,[38] Ag_n nanoparticle formation,[37] protein aggregation in at least some of the major neurological diseases,[39,40] gelatin R1 renaturation,[36] and H_2SO_4 nucleation in atmospheric chemistry[41]—already a rather broad cross section of phase changes across nature. Noteworthy here is that these hints of the broader generality of bimolecular to termolecular nucleation encompass relatively weak bonding/associating chemical interactions such as those present in the protein aggregation and H_2SO_4 nucleation systems.
- Worth mentioning here is that there is also computational evidence for bimolecular nucleation as a preferred process in water condensation in expanding/cooling water plumes[69] and of simulated nucleation populations that drop off by $\sim 10^{7.5}$ as one goes from dimers to 10-mers in a glassy solid crystallization system.[70] The protein aggregation simulations by Stryer come to mind here as well, Stryer showing that dimer formation is favored over all other aggregates in the monomer-addition mechanism[39] since only the dimer grows with a quadratic dependence on [A].[71] There is, therefore, every reason to expect that rate-limiting bimolecular to perhaps termolecular nucleation may well apply rather broadly to other systems across nature. In short, the rate-determining second-order nucleation uncovered in the present work should serve as one key starting hypothesis for attempted disproof in future studies of the reaction order and implied molecularity of nucleation phenomena across nature.
- The FOC is an additional needed, new concept that has, therefore, also been postulated as part of this work. Prior literature claims of observation of the putative "critical nucleus" of CNT are, instead, very likely to have actually detected the FOC due to limitations in the sensitivity or time-resolution of even the most powerful physical methods used to date.
- The demonstrated applicability of the unimolecular form of the FW two-step mechanism (and thus by analogy to the present work its equivalently equally well-fitting bimolecular form) to other areas such as heterogeneous catalyst formation,[51] protein aggregation,[39,40] and solid-state reactions[32] implies that the hypothesis of the bimolecular FW two-step mechanism merits careful scrutiny as a first minimal mechanism for curve-fitting of kinetic data in other systems. The FW two-step mechanism is analogously a good first choice for kinetic simulations as well. Use of the FW two-step mechanism in its unimolecular form is easiest and should suffice for the purposes of data fitting in most cases and where the precursor concentration, [A], is effectively constant during the nucleation period.
- The nine insights, predictions, and synthetic implications of the FW two-step mechanism, reproduced in a footnote herein for the interested reader,[32] are still valid in light of the finding herein of second-order nucleation. However, the new insight is that second-order nucleation provides an increased degree of separation of nucleation from autocatalytic growth. That degree of separation is important in achieving the typically $\leq \pm 15\%$, by definition near-monodisperse,[49] size distributions commonly observed when the FW-two-step mechanism fits the observed kinetic data.
- The availability of the second-order FW two-step mechanism herein is important in a broader, more fundamental context. Specifically, such disproof-based, minimalistic, elementary, or pseudo-elementary step mechanisms are the required, necessary foundation—the crucial underpinning—that enables the needed, more sophisticated, more complex "physical" or "engineering" models of phenomenon across nature such as nucleation, growth, and agglomeration. However, to be reliable we assert that those needed, more complex models must start from, incorporate and overall build off of disproof-based mechanistic models.
- The limitations of the FW two-step mechanism have also been cited[33] and derive from the still too simple nature of this mechanistic model and the average nanoparticle rate constants, average size, and other average properties and insights that it yields. The lack of any information about the nanoparticle size distribution (ideally as a function of time) is a major shortcoming of the FW two-step model as we have previously noted.[50] Hence, improvements and more complex models, that employ the FW two-step model as their starting foundation and thus build off and improve the FW two-step model, are both needed and welcomed.[72]
- An additional implication of this work is that LaMer's highly cited, but actually relatively little supported, "burst nucleation and diffusion controlled growth" physical model for sulfur sol formation from the 1950s[11] needs to be critically reexamined.[73] This assertion follows since LaMer's model is based in part on CNT and makes the assumption of "burst" nucleation. Lamer's model is, therefore, likely simply not correct for at least systems and nanoparticle syntheses not performed by the hot-injection method. This assertion is supported by the many failed attempts to use quantitatively, and thereby support, LaMer's model during the now 60+ intervening years.[11] It, like CNT, is as Turkevich noted 63 years ago

dx.doi.org/10.1021/ja510263s | J. Am. Chem. Soc. 2014, 136, 17601−17615

a "theory of great tradition",[74] but one who's time for reassessment has now come.

- Significantly, now that the correct, minimal, elementary step of continuous second-order nucleation and the pseudo-elementary step of autocatalyic growth are in hand, mechanistically underpinned efforts to describe and model nanoparticle size distributions vs time can be rationally approached. Those efforts will supplant recent useful, but conceptually flawed, studies where a mechanism is assumed prior to the, for example, population balance modeling and simulations.[75] Such studies which do not start from a well-established chemical mechanism only create controversy and confusion and should be avoided in our opinion.
- One among other crucial benefits of building from the relatively firm foundation of mechanistic, disproof-based models is that doing so incorporates naturally the proper specific words (and associated rate constants) to describe the phenomenon at hand. This occurs naturally since the balanced elementary or pseudo-elementary steps of mechanistic models define the needed, specific words and concepts. An excellent example is the now unequivocally defined continuous second-order nucleation and autocatalytic growth steps of the second-order nucleation FW two-step mechanism. The associated concepts of a KEN and FOC follow. The disconnect present in nonmechanistic models, between the differential equations given and the words then tacked on *ad hoc* to describe the physical processes at hand, continues to be a persistent, conceptually confusing, controversy generating and thus progress-inhibiting aspect of purely physical or engineering models of dynamic processes across nature.[35]
- Next and very importantly, these studies begin to offer some insights and clarity into when CNT should be used and when it is simply not applicable. For simple, $n\mathrm{A} \rightarrow \mathrm{A}_n$ systems with gas-phase hydrocarbon droplet formation being a prototype example,[17] CNT and its equilibrium-based treatment and critical nucleus concept and language are applicable and do provide a reasonable job of describing the physical process at hand in these low supersaturation systems. However, in systems that involve other reagents and can proceed via other intermediates, changed oxidation states, or other more facile kinetic pathways than that provided by simple aggregation of $n\mathrm{A} \rightarrow \mathrm{A}_n$, CNT is best viewed as simply not applicable in our opinion. The current prototype example is the $2\mathrm{A}\ (\mathrm{Ir}^{\mathrm{I}}) + \mathrm{H}_2 \rightarrow \{\mathrm{Ir}_2\mathrm{H}_2\} \rightarrow\rightarrow \mathrm{B}\ (\mathrm{Ir}^0_n)$ system herein implied (but not unequivocally demonstrated, *vide infra*) by the present studies. The concepts of the KEN and FOC should be used in such cases, not the critical nucleus and other language and concepts of CNT.
- Finally, despite the insights and new concepts of the KEN and FOC provided by the present studies, we wish to emphasize that the still (and by-design) minimalistic second-order nucleation FW two-step mechanism detailed herein is almost surely not the final, true, more intimate nucleation mechanism in many, if not most cases, that begin with complex nanoparticle precursors that are not the actual assembling A. Additional studies beyond the scope of the present work are needed to distinguish, for example, bimolecular from termolecular mechanisms that we have been able to write, both of which can show net second-order kinetics—why we have been careful in the present work to distinguish and use where appropriate the distinct concepts of empirical reaction order vs that of the intimate mechanism-derived, theoretical molecularity of a postulated, underlying elementary step. All the rate constants such as $k_{1\mathrm{obs(bimol)}}$ or KEN = 2 obtained herein are, therefore and as already noted, apparent rate constants and an apparent KEN. Mechanistic science is by its very nature stepwise, cautious, and highly evolutionary, building piece-by-piece and step-by-step to more complex mechanisms, but only as the data demand! In addition, even for relatively simple bi- to termolecular nucleations, possible $\mathrm{Ir}(0)_2$, $\mathrm{Ir}_2\mathrm{H}$, $\mathrm{Ir}_2\mathrm{H}_2$, Ir_2^+, $\mathrm{Ir}_2\mathrm{H}^+$ or $\mathrm{Ir}(0)_3$, $\mathrm{Ir}_3\mathrm{H}$, $\mathrm{Ir}_3\mathrm{H}_2$, $\mathrm{Ir}_3\mathrm{H}_3$, Ir_3^+, $\mathrm{Ir}_3\mathrm{H}^+$ and other possible, nominal compositions of the activated complex of the rate-determining, nucleation step also remain as important hypotheses awaiting experimental scrutiny and attempted disproof. In that sense, the present contribution is quite modest in some sense, yet arguably profound and possibly (if not probably) far reaching in another sense simply due to its demonstration of simple second-order, and not higher order, nucleation with a the KEN of 2−3, but not the larger "critical nucleus" implied by CNT, for a transition-metal nanocluster formation system. The needed additional studies are continuing and will be reported in due course.

■ ASSOCIATED CONTENT

Supporting Information

Derivations for the integrated rate equations used to fit the kinetic data. Additional mechanistic data from the "*in-situ* formed" catalyst reactions are also provided for the interested reader. This material is available free of charge via the Internet at http://pubs.acs.org.

■ AUTHOR INFORMATION

Corresponding Author

rfinke@lamar.colostate.edu

Notes

The authors declare no competing financial interest.

■ ACKNOWLEDGMENTS

Support from DOE grant 5338080 to R.G.F. is gratefully acknowledged. We thank Dr. Lisa Starkey-Ott for her early experimental work suggesting that nucleation was second-order based on *in situ* prepared precatalyst as shown in the Supporting Information and Professor M. S. El-Shall for sharing his expert insights into CNT when asked to read the penultimate draft of this paper.

■ REFERENCES

(1) Kashchiev, D. *Nucleation: Basic Theory with Applications*; Butterworth-Heinemann: Oxford, U.K., 2000.

(2) Sipilä, M.; Berndt, T.; Petäjä, T.; Brus, D.; Vanhanen, J.; Stratmann, F.; Patokoski, J.; Mauldin, R. L.; Hyvärinen, A.-P.; Lihavainen, H.; Kulmala, M. *Science* **2010**, *327*, 1243−1246.

(3) Chen, S.; Ferrone, F. A.; Wetzel, R. *Proc. Natl. Acad. Sci. U.S.A.* **2002**, *99*, 11884−11889.

(4) Dauer, W.; Przedborski, S. *Neuron* **2003**, *39*, 889−909.

(5) Zhang, T. H.; Liu, X. Y. *Angew. Chem., Int. Ed.* **2009**, *48*, 1308−1312.

(6) Finney, E. E.; Finke, R. G. *J. Colloid Interface Sci.* **2008**, *317*, 351−374.
(7) *Clusters and colloids. From Theory to Applications*; Seifert, G., Schmid, G., Eds.; VCH Verlagsgesellschaft: Weinheim, 1994.
(8) Volmer, M.; Weber, A. Z. *Phys. Chem. (Leipzig)* **1926**, *119*, 227.
(9) Volmer, M. *Kinetik der Phasenbildung*; Steinfopff: Leipzig, 1939.
(10) Becker, R.; Döring, W. *Ann. Phys.* **1935**, *24*, 719.
(11) LaMer, V. K.; Dinegar, R. H. *J. Am. Chem. Soc.* **1950**, *72*, 4847.
(12) Moore, J. W.; Pearson, R. G. *Kinetics and Mechanism*, 3rd ed.; Wiley-Interscience: New York, 1981; p 226, Table 6.8.
(13) Oxtoby, D. W. *J. Phys.: Condens. Matter* **1992**, *4*, 7627−7650.
(14) Dixit, N. M.; Zukoski, C. F. *Phys. Rev. E* **2002**, *66*, 051602.
(15) Lubetkin, S. D. *Langmuir* **2003**, *19*, 2575.
(16) Erdemir, D.; Lee, A. Y.; Myerson, A. S. *Acc. Chem. Res.* **2009**, *42*, 621. Note that the pictorial "two-step model" in this valuable review (i.e., and involving a meta-stable, disordered, proposed-intermediate phase in crystal formation from solution) is not the FW two-step mechanism employed herein. However, also worth noting is that the FW two-step mechanism has been used to fit such solid-state formation kinetic data in other systems[32] and, therefore, is a kinetic model that can be used for actual attempted fitting of such data.
(17) (a) Rusyniak, M.; Abdelsayed, V.; Campbell, J.; El-Shall, M. S. *J. Phys. Chem. B* **2001**, *105*, 11866. (b) Rusyniak, M.; El-Shall, M. S. *J. Phys. Chem. B* **2001**, *105*, 11873. (c) Abedalsayed, V.; Ibrahim, Y.; Rusyniak, M.; Rabeony, M.; El-Shall, M. S. *J. Chem. Phys.* **2001**, *115*, 2897.
(18) Zhang, T. H.; Liu, X. Y. *Angew. Chem., Int. Ed.* **2009**, *48*, 1308−1312 and references therein.
(19) Li, Z.; Cheng, H.; Han, C. C. *Macromolecules* **2012**, *45*, 3231−3239.
(20) Oxtoby, D. W. *Acc. Chem. Res.* **1998**, *31*, 91.
(21) Gasser, U.; Weeks, E. R.; Schofield, A.; Pusey, P. N.; Weitz, D. A. *Science* **2001**, *292*, 258−262.
(22) (a) CNT is also stated to be incompatible with the growing evidence for so-called "prenucleation" clusters,[22b] although the needed kinetic evidence, to know where such observable clusters actually fit into the true mechanism of nucleation of crystallizing systems, is lacking at present. (b) Gebauer, D.; Kellermeier, M.; Gale, J. D.; Bergström, L.; Cölfen, H. *Chem. Soc. Rev.* **2014**, *43*, 2348−2371. (c) Amabilino, D. B.; Obradors, X. *Chem. Soc. Rev.* **2014**, *43*, 2009−2012. This accompanying editorial[22b] is telling reading about the current, poorly understood status of nucleation in the challenging area of crystallization processes, noting that the questions of "where nuclei come from?" and "what is their nature?" continue to "taunt scientists", "despite our incredible analytical tools and computer power".
(23) For example, the first row, and hence relatively weak, Mn−Mn bond energy is fairly well determined and is ∼38 kcal/mol, see p. 240, Table 4.1 of: Collman, J. P.; Hegedus, L. S.; Norton, J. R.; Finke, R. G. *Principles and Applications of Organotransition Metal Chemistry*; University Science Books, Mill Valley, CA, 1987.
(24) Martinho Simoes, J. A.; Beauchamp, J. L. *Chem. Rev.* **1990**, *90*, 629−688.
(25) This rough, expected to be lower limit estimate of the Ir(0)−Ir(0) bond energy in a small particle can be obtained by taking the $\Delta H_{\text{Vaporization}}$ of Ir metal of $\Delta H_{\text{Vaporization}}$ = 159 kcal/mol and dividing by the Ir coordination number in the solid of 12 divided by 2 (two Ir for each Ir−Ir), that is, 159/(12/2) = 26 kcal/mol. Since there is a well-known contraction of the Ir−Ir distance on at least the surface of small Metal(0)$_n$ nanoparticles, one expects that this 26 kcal/mol value is probably a lower limit to the true Ir(0)−Ir(0) bond energy in small Ir(0)$_n$ particles. Ligation of the Ir(0) will, of course, result in additional changes to the Ir(0)−Ir(0) in a given, [Ir(0)]$_n$(Ligand)$_m$ system.
(26) Noteworthy here is the importance of the reversibility of an M_n + $(x{\cdot}m)$L to M_{n-m} + mML$_x$ equilibrium in determining if a reaction is catalyzed by a homogeneous vs a heterogeneous catalyst: Widegren, J. A.; Finke, R. G. *J. Mol. Catal. A.: Chemical* **2003**, *198*, 317−341 see the last bullet point on p. 334.
(27) It is known that growth of an Ir$_1$·zeolite Y system to Ir$_4$·zeolite Y is favored under H_2 but reverses under ethylene, although the ligating effects of the zeolite Y support are presumably significant in this heterogeneous catalyst system, see: Uzun, A.; Gates, B. C. *J. Am. Chem. Soc.* **2009**, *131*, 15887−15894.
(28) For the synthesis, crystallization and crystallographic, XAFS and other characterization of a Ir_4H_4(1,5-COD)$_4$ subnanometer cluster that rapidly reacts under H_2, see: Yih, K.-H.; Hamdemir, I. K.; Mondloch, J. E.; Bayram, E.; Özkar, S.; Vasic, R.; Frenkel, A. I.; Anderson, O. P.; Finke, R. G. *Inorg. Chem.* **2012**, *51*, 3186−3193.
(29) Watzky, M. A.; Finke, R. G. *J. Am. Chem. Soc.* **1997**, *119*, 10382−10400.
(30) Watzky, M. A.; Finke, R. G. *Chem. Mater.* **1997**, *9*, 3083−3095.
(31) (a) The concept of pseudo-elementary steps was introduced in the 1970s by Noyes, who developed this concept using kinetic studies of complex oscillating reactions. By pseudo-elementary we mean collections of one or more slow steps, plus any number of faster steps, that when added together yield a balanced reaction that can be uses as effectively elementary (i.e., as pseudo-elementary) for the purposes of kinetic treatments in the same way that truly elementary steps are used as the basic building blocks of reliable reaction mechanisms. That said, the reaction order of a pseudo-elementary step cannot be directly used to imply the molecularity of that (composite) step as is the case with a true elementary step. (b) Noyes, R. M.; Field, R. J. *Acc. Chem. Res.* **1977**, *10*, 214−221.
(32) Finney, E. E.; Finke, R. G. *Chem. Mater.* **2009**, *21*, 4692. The nine insights from the FW two-step mechanism are listed in the this publication, insights reproduced below for the interested reader (please see this publication for the references cited therein in support of the insights listed below): (i) Understanding how to form routinely near-monodisperse (defined as $\leq \pm 15\%$)[49] size distributions of typically "magic-number sized" (i.e., full shell) size distributions of supported nanoclusters due to a significant separation of nucleation from growth in time; (ii) a start on rational size control via a mechanism-based nanocluster size vs time equation in terms of k_1, k_2, the precatalyst concentration, $[A]_0$, and N*; (iii) additional possible size control via olefin or other ligand dependence; (iv) rational use of seeded-growth methods as a result of autocatalytic surface-growth including the rational synthesis of all possible geometric isomers of multimetallic "nano-onions"; (v) rational catalyst shape control via ligands capable of attaching to the growing nanocluster faces and thereby preventing autocatalytic surface growth of that facet; (vi) knowledge of the negative effects of, and insights into how to avoid, mass-transfer limitations in nanocluster syntheses; (vii) knowledge of what added nanocluster surface ligands can provide additional nanocluster stability if desired; (viii) key components of a ranking system for nanocluster stabilizers; and (ix) the possibility of nanocluster size-dependent surface metal-to-ligand bond energies plus all that intriguing preliminary finding implies for catalysis.
(33) Kent, P. D.; Mondloch, J. E.; Finke, R. G. *J. Am. Chem. Soc.* **2014**, *136*, 1930−1941 see the section on "Limitations of the Four-Step Mechanism", and refs 24, 27−30 and 31 listed therein.
(34) Finney, E. E.; Finke, R. G. *Chem. Mater.* **2009**, *21*, 4692−4705 and references cited therein.
(35) Finney, E. E.; Finke, R. G. *Chem. Mater.* **2009**, *21*, 4468−4479. See the section in the SI titled: "Some Useful References and Comments on Models in Science".
(36) Busnel, J. P.; Morris, E. R.; Ross-Murphy, S. B. *Int. J. Biol. Macromol.* **1989**, *11*, 119−125. The reaction order these authors found in the starting gelatin R1 was ∼2.2.
(37) (a) Evidence for Ag_2^+: Henglein, A.; Giersig, M. *J. Phys. Chem. B* **1999**, *103*, 9533−9539. (b) Evidence for Ag(0)$_2$, but where the authors considered and believe they can rule out, a Ag(0) + Ag + to Ag_2^+ step: Stamplecoskie, K. G.; Scaiano, J. C. *J. Am. Chem. Soc.* **2011**, *133*, 3913−3920.
(38) Yao, S.; Yuan, Y.; Xiao, C.; Li, W.; Kou, Y.; Dyson, P. J.; Yan, N.; Asakura, H.; Teramura, K.; Tanaka, T. *J. Phys. Chem. C* **2012**, *116*, 15076−15086.
(39) Morris, A. M.; Watzky, M. A.; Agar, J. N.; Finke, R. G. *Biochemistry* **2008**, *47*, 2413−2427.

(40) Meisl, G.; Yang, X.; Hellstrand, E.; Frohm, B.; Kirkegaard, J. B.; Cohen, S. I. A.; Dobson, C. M.; Linse, S.; Knowles, T. P. J. *Proc. Natl. Acad. Sci. U. S. A.* **2014**, *111*, 9384−9389.
(41) (a) Zhang, R. *Science* **2010**, *328*, 1366−1367. See the interesting discussion therein—discussion highly relevant to the concepts proposed herein of a KEN and first-observable cluster—of the most recent nucleation studies by more sensitive methods that suggest a "critical nucleus" for H_2SO_4 droplet nucleation of 2 (what we call herein a KEN). Note also the discussion therein pointing out that prior studies (by less sensitive methods) previously reported a "critical nucleus" of four-to-nine, $(H_2SO_4)_{4-9}$, that "agreed with predictions from classical nucleation theory", but apparently missed the true (kinetically effective) nucleus and are, instead, what we define herein the first-observable cluster(s). (b) Sipilä, M.; Berndt, T.; Petäjä, T.; Brus, D.; Vanhanen, J.; Stratmann, F.; Patokoski, J.; Mauldin, R. L., III; Hyvärinen, A.-P.; Lihavainen, H.; Kulmala, M. *Science* **2010**, *327*, 1243−1246.
(42) Atmospheric nucleation is obviously complex, as the following paper detailing the large effects of NH_3 on atmospheric H_2SO_4 nucleation demonstrate: Kirkby, J.; Curtius, J.; Almeida, J.; Dunne, E.; Duplissy, J.; Ehrhart, S.; Franchin, A.; Gagné, S.; Ickes, L.; Kürten, A.; Kupc, A.; Metzger, A.; Riccobono, F.; Rondo, L.; Schobesberger, S.; Tsagkogeorgas, G.; Wimmer, D.; Amorim, A.; Bianchi, F.; Breitenlechner, M.; David, A.; Dommen, J.; Downard, A.; Ehn, M.; Flagan, R. C.; Haider, S.; Hansel, A.; Hauser, D.; Jud, W.; Junninen, H.; Kreissl, F.; Kvashin, A.; Laaksonen, A.; Lehtipalo, K.; Lima, J.; Lovejoy, E. R.; Makhmutov, V.; Mathot, S.; Mikkilä, J.; Minginette, P.; Mogo, S.; Nieminen, T.; Onnela, A.; Pereira, P.; Petäjä, T.; Schnitzhofer, R.; Seinfeld, J. H.; Sipilä, M.; Stozhkov, Y.; Stratmann, F.; Tomé, A.; Vanhanen, J.; Viisanen, Y.; Vrtala, A.; Wagner, P. E.; Walther, H.; Weingartner, E.; Wex, H.; Winkler, P. M.; Carslaw, K. S.; Worsnop, D. R.; Baltensperger, U.; Kulmala, M. *Nature* **2011**, *476*, 429−433.
(43) Henglein, A.; Giersig, M. *J. Phys. Chem. B* **2000**, *104*, 6767−6772.
(44) Harada, M.; Kamigaito, Y. *Langmuir* **2012**, *28*, 2415−2428.
(45) Yih, K.-H.; Hamdemir, I. K.; Mondloch, J. E.; Bayram, E.; Özkar, S.; Vasic, R.; Frenkel, A. I.; Anderson, O. P.; Finke, R. G. *Inorg. Chem.* **2012**, *51*, 3186−3193. See also the list therein of other known M_4 clusters.
(46) Bayram, E.; Linehan, J. C.; Fulton, J. L.; Roberts, J. A. S.; Szymczak, N. K.; Smurthwaite, T. D.; Özkar, S.; Balasubramanian, M.; Finke, R. G. *J. Am. Chem. Soc.* **2011**, *133*, 18889−18902.
(47) Duff, D. G.; Curtis, A. C.; Edwards, P. P.; Jefferson, D. A.; Johnson, B. F. G.; Logan, D. E. *J. C. S. Chem. Comm.* **1987**, 1264−1266.
(48) (a) Amir, H.-A.; Engel, M.; Keys, A. S.; Zheng, X.; Petschek, R. G.; Palffy-Muhoray, P.; Glotzer, S. C. *Nature* **2009**, *462*, 773−777. (b) Chen, E. R.; Engel, M.; Glotzer, S. C. *Condensed Matter* **2010**, 1−26.
(49) Finke, R. G. In *Metal Nanoparticles: Synthesis, Characterization and Applications*; Feldheim, D. L.; Foss Jr., C. A., Eds.; Marcel Dekker, Inc.: New York, 2002, Chapter 2, pp 17−54.
(50) Watzky, M. A.; Finney, E. E.; Finke, R. G. *J. Am. Chem. Soc.* **2008**, *130*, 11959−11969.
(51) Mondloch, J. E.; Finke, R. G. *ACS Catal.* **2012**, *2*, 298−305.
(52) Mondloch, J. E.; Finke, R. G. *J. Am. Chem. Soc.* **2011**, *133*, 7744−7756.
(53) Besson, C.; Finney, E. E.; Finke, R. G. *J. Am. Chem. Soc.* **2005**, *127*, 8179.
(54) Özkar, S.; Finke, R. G. *J. Am. Chem. Soc.* **2002**, *124*, 5796−5810.
(55) $Ir(0)_{\sim 300}$ nanoparticles formed at 1.2 mM standard conditions. Nanoparticle size increases at higher concentration of catalyst precursor and range from ∼1.8(±0.2) nm to 3.4(±0.5) nm for smples in this study.
(56) Day, V. W.; Klemperer, W. G.; Main, D. J. *Inorg. Chem.* **1990**, *29*, 2345−2355.
(57) Weiner, H.; Aiken, J. D.; Finke, R. G. *Inorg. Chem.* **1996**, *35*, 7905−7913.
(58) Mbomekalle, I.-M.; Lu, Y. W.; Keita, B.; Nadjo, L. *Inorg. Chemistry Commun.* **2004**, *7*, 86−90.
(59) Graham, C. R.; Finke, R. G. *Inorg. Chem.* **2008**, *47*, 3679−3686.
(60) Randall, W. J.; Droege, M. W.; Mizuno, N.; Nomiya, K.; Weakley, T. J. R.; Finke, R. G.; Isern, N.; Salta, J.; Zubieta, J. *Inorg. Synth.* **1997**, *31*, 167−185.
(61) Laxson, W. W.; Özkar, S.; Finke, R. G. *Inog. Chem.* **2014**, *53*, 2666−2676.
(62) Finke, R. G.; Droege, M. W.; Domaille, P. J. *Inorg. Chem.* **1987**, *26*, 3886−3896.
(63) Pohl, M.; Lyon, D. K.; Mizuno, N.; Nomiya, K.; Finke, R. G. *Inorg. Chem.* **1995**, *34*, 1413−1429.
(64) In our prior, initial work testing for second-order nucleation when beginning with a (1,5-COD)IrCl·γ-Al_2O_3 heterogeneous precatalyst system,[51] the correction factors for $k_{2obs(curvefit)}$ and $k_{1obs(bimol,curvefit)}$ were erroneously reported as different by a factor of 2. This error resulted from incompatible definitions of the k_{1obs} and $k_{1obs(bimol)}$ rate constants in that paper's equations S12 and S14, an error and definition that are hereby corrected via the equations S11 and S13 in the SI of the present paper.
(65) Platt, J. R. *Science* **1964**, *146*, 347−353.
(66) Lin, Y.; Finke, R. G. J. *Am. Chem. Soc.* **1994**, *116*, 8335−8353.
(67) Strey, R.; Wagner, P. E.; Viisanen, Y. *J. Phys. Chem.* **1994**, *98*, 7748.
(68) (a) See for example the following state-of-the-art paper,[68b] on isonicotinamide crystallization from 700 rpm-stirred EtOH, in which 144 repeat heat/cooling to 25 °C cycles of crystallization are followed for a given sample in this weakly bonded system using a "Crystal16" multiple sample reactor that detects turbidity by measuring light transmission through the sample. In that work, dust particles—and resultant heterogeneous nucleation—are shown to dominate >two-thirds of the data. They report a "nucleus size", $n^* = 11-50$, but note that what they are actually monitoring is the first-observable cluster, as defined herein, via their light-transmission threshold value, yielding solid product that is formed predominantly as a result of dust-initiated, heterogeneous nucleation. (b) Kulkarni, S. A.; Kadam, S. S.; Meekes, H.; Stankiewicz, A. I.; ter Horst, J. H. *Cryst. Growth Des.* **2013**, *13*, 2435−2440.
(69) Li, Z.; Zhong, J.; Levin, D. A.; Garrison, B. J. *J. Chem. Phys.* **2009**, *130*, 174309.
(70) Lee, B.-S.; Burr, G. W.; Shelby, R. M.; Raoux, S.; Rettner, C. T.; Bogle, S. N.; Darmawikarta, K.; Bishop, S. G.; Abelson, J. R. *Science* **2009**, *326*, 980−984. See Figure 3 therein.
(71) Goldstein, R. F.; Stryer, L. *Biophys. J.* **1986**, *50*, 583−599 Stryer makes a comment on p. 593 based on his results and earlier results of others regarding nucleation, a comment that strikes a cord in light of our current second-order nucleation studies, "...the pre-equilibrium assumption is highly suspect···". "Why was this not discovered earlier?".
(72) (a) A recent reference in this regard is the paper by Kumar, et al.[72b] which adds population balance (PB) modeling to the FW two-step mechanism to try to account for the relatively narrow, ≤±15% nanoparticle size distributions typically seen when the FW two-step mechanism fits the nanoparticle formation kinetic data. However and unfortunately, that paper: (i) only examines one limited data set digitized from our original literature (i.e., so that the high precision of the original data is lost for the subsequent curve-fitting); (ii) does not know, and therefore fails to consider, the true intimate mechanism of nucleation—a major weakness since nucleation is the step(s) that the study is trying to understand; (iii) fails to consider a range of known mechanisms that could explain the data; (iv) fails to consider a stochastic approach to the size distribution problem; (v) then adds, in an ad hoc and thus nonmechanistic way, what ultimately is a solubility-based "burst" nucleation in their "PBM-4s" model in place of the now known, second-order, continuous nucleation; and (vi) fails to present and discuss in the main text any of the assumptions and approximations in the PB modeling and how they might influence the paper's conclusions. Hence, (vii) the primary conclusion in this PB modeling paper, that nucleation must somehow be "delayed", cannot

be trusted at present. Required is more careful scrutiny and testing via PB modeling once we have finished elucidating and report the more intimate mechanism of nucleation underlying the FW two-step model, that correct chemical mechanism being the presently missing, but required input, for reliable PB modeling. (b) Perala, S. R. K.; Kumar, S. *Langmuir* **2014**, *30*, 12703−12711.

(73) We are working on just such a needed, critical reanalysis of LaMer's mechanism and its evidence, including literature that claims to use and support LaMer's mechanism. We will report on that effort in due course.

(74) Turkevich, J.; Stevenson, P. C.; Hillier, J. *Discuss. Faraday Soc.* **1951**, *11*, 55.

(75) Perala, S. R. K.; Kumar, S. *Langmuir* **2013**, *29*, 9863−9873. This paper assumes CNT for modeling nucleation, assumes a mechanism, assumes (somewhat randomly, and almost surely incorrectly) a nucleus of Au_{10}, and then uses a population balance model that has 10 parameters to purportedly rule out the burst nucleation mechanism of LaMer. The paper then claims to support what is worded and implied to be novel as a "continuous nucleation growth passivation based mechanism", but the paper does not offer any compelling evidence for "continuous nucleation" since that step is basically input as an assumption in their (assumed) mechanism. In addition, since continuous nucleation was first reported by Watzky 16 years earlier,[50] one should ignore these author's ill-advised, implied claim of novelty for their proposed "continuous nucleation".